

Article

Supercritical Direct-Methane-to-Methanol Coupled with Gas-to-Wire for Low-Emission Offshore Processing of CO₂-Rich Natural Gas: Techno-Economic and Thermodynamic Analyses

Alessandra de Carvalho Reis, Ofélia de Queiroz Fernandes Araújo  and José Luiz de Medeiros * 

Escola de Química, Federal University of Rio de Janeiro, CT, E, Ilha do Fundão, Rio de Janeiro 21941-909, RJ, Brazil; alessandracr@eq.ufrj.br (A.d.C.R.); ofelia@eq.ufrj.br (O.d.Q.F.A.)

* Correspondence: jlm@eq.ufrj.br

Abstract: A greater H/C ratio and energy demand are factors that boost natural gas conversion into electricity. The Brazilian offshore pre-salt basin has large reserves of CO₂-rich associated gas. Selling this gas requires high-depth long-distance subsea pipelines, making gas-to-pipe costly; in particular, gas-to-wire instead of gas-to-pipe is more practical since it is easier to transmit electricity via long subsea distances. This research proposes and investigates an innovative low-emission gas-to-wire alternative consisting of installing supercritical direct-methane-to-methanol upstream to gas-to-wire, which is embedded in an exhaust-gas recycle loop that reduces the subsequent carbon capture costs. The process exports methanol and electricity from remote offshore oil-and-gas fields with available CO₂-rich natural gas, while capturing CO₂. Techno-economic, thermodynamic and lost work analyses assess the alternative. Supercritical direct-methane-to-methanol is conducted in supercritical water with air. This route is chosen because supercritical water readily dissolves methanol and CO₂, helping to preserve methanol via stabilization against further oxidation by gaseous air. Besides being novel, this process has intensification since it implements exhaust-gas recycle for –flue-gas reduction, CO₂ abatement via post-combustion capture with aqueous monoethanolamine, CO₂ dehydration with triethylene glycol and CO₂ densification for enhanced oil recovery. The process is fed with 6.5 MMS m³/d of CO₂-rich natural gas (CO₂ > 40%mol) exporting methanol (2.2 t/h), electricity (457.1 MW) and dense CO₂ for enhanced oil recovery, with an investment of 1544 MMUSD, 452 MMUSD/y in manufacturing costs and 820 MMUSD/y in revenues, reaching 1021 MMUSD net present value (50 years) and a 10 year payback time. The Second Law analysis reveals overall thermodynamic efficiency of 28%. The lost work analysis unveils the gas-combined-cycle sub-system as the major lost work sink (76% lost work share), followed by the post-combustion capture plant (14% lost work share), being the units that prominently require improvements for better economic and environmental performance. This work demonstrates that the newly proposed process is techno-economically feasible, environmentally friendly, thermodynamically efficient and competitive with the gas-to-wire processes in the literature.

Keywords: direct methane-to-methanol; supercritical water; gas-to-wire; natural gas combined cycle; post-combustion carbon capture; CO₂ dehydration; thermodynamic analysis



Citation: Reis, A.d.C.; Araújo, O.d.Q.F.; de Medeiros, J.L. Supercritical Direct-Methane-to-Methanol Coupled with Gas-to-Wire for Low-Emission Offshore Processing of CO₂-Rich Natural Gas: Techno-Economic and Thermodynamic Analyses. *Processes* **2024**, *12*, 374. <https://doi.org/10.3390/pr12020374>

Academic Editors: Bahaa Saleh and Fadl A. Essa

Received: 16 January 2024

Revised: 7 February 2024

Accepted: 10 February 2024

Published: 13 February 2024



Copyright: © 2024 by the authors. Licensee MDPI, Basel, Switzerland. This article is an open access article distributed under the terms and conditions of the Creative Commons Attribution (CC BY) license (<https://creativecommons.org/licenses/by/4.0/>).

1. Introduction

Fossil fuels still lead the global energy matrix, despite the increasing utilization of renewable sources. A huge rise in power generation from natural gas is predicted for the next few decades, considering that natural gas (NG) is the cleanest fossil fuel and its reserves are expanding [1]. In the Brazilian pre-salt offshore basin, the deep-water oil reserves have a high gas-to-oil ratio with an associated gas that is very rich in terms of carbon dioxide (CO₂) (above 40%mol) [2]. The commercialization of this low-quality gas requires large investments in high-depth long-distance subsea pipelines to deliver

such NG to the market [3]. In this context, a suitable solution to overcome both the NG and CO₂ transport infrastructures (gas-to-pipe) is to implement floating gas-to-wire (GTW) plants comprising NG combined cycles (NGCC) [4]. An important issue for the technical feasibility of GTW is the gas availability in order to guarantee its conversion into electricity [5]. Implemented on floating rigs over offshore gas fields, GTW converts the raw gas directly into electricity, which is sent to onshore sites by using high-voltage direct-current (HVDC) cables [6] for lower transmission losses [7]. However, GTW per se is not sufficient given the current climate concerns, i.e., GTW must be accompanied by carbon capture and storage (CCS) or carbon capture and utilization (CCU) in order to guarantee low CO₂ emissions.

1.1. Offshore Gas-to-Wire with CCS

Given the global warming scenario, GTW must be combined with CCS or CCU to reach emission targets [8], lowering the carbon footprint of the produced power [9]. A suitable solution for the captured CO₂ is its reinjection into the reservoir as enhanced oil recovery (EOR) fluid [10], since it increases oil production [11], offering additional monetary leverage [12]. Thus, EOR is considered a CCU strategy. Assessing several CCS configurations (such as chemical absorption, physical absorption, membrane permeation and hybrids), Araújo et al. [13] identified that chemical absorption attains the minimum CO₂ emissions per ton of CO₂ injected. Hetland et al. [14] studied a GTW-CCS plant evaluating the coupling of post-combustion carbon capture (PCC) with a floating Siemens NGCC. In their configuration, the NGCC flue gas feeds a PCC unit using an aqueous monoethanolamine (aqueous MEA) solvent. Despite not considering important techniques like exhaust gas recycling (EGR) and CO₂-EOR stream dehydration, the authors demonstrated the theoretical feasibility of a floating GTW-CCS.

In the context of low-emission GTW-CCS processes, EGR is being considered in the literature [15]. EGR favors the CO₂ separation step, since it lowers the exhaust gas flow rate and raises the flue gas CO₂ content. Higher CO₂ content increases the driving force for CO₂ capture, decreasing the column height, while the lower flue gas flow rate lowers the column diameter, i.e., both EGR consequences reduce the CCS/CCU investment [16]. As the circulating nitrogen and oxygen flow rates diminish in the flue gas, EGR also reduces NO_x emissions [17]. Thus, GTW-CCS implementation on offshore rigs over deep-water oil-and-gas fields must consider (i) EGR; (ii) post-combustion carbon capture from enriched flue gas through absorption in aqueous monoethanolamine (aqueous MEA), i.e., the PCC-MEA plant; (iii) a high-pressure CO₂ dehydration unit (CDU) to reduce the water content (below ≈160 ppm-mol), preventing CO₂ hydrate formation [18]; and (iv) the injection of dense CO₂ in the reservoir as an EOR agent.

1.2. Direct Methane-to-Methanol

Direct methane (conversion) to methanol (DMTM) has been widely investigated in the literature as an alternative for the production of methanol from methane, dismissing the expensive reforming and synthesis gas route. Zakaria and Kamarudin [19] discuss several pathways for DMTM, including gas-phase DMTM, liquid-phase DMTM and supercritical DMTM. Zhang et al. [20] carried out gas-phase DMTM, obtaining methanol selectivity of 60% at 13% methane conversion at 50 bar and 430–470 °C. Holmen [21] also studied gas-phase DMTM and claimed that the best results occurred at methanol selectivity values of 30–40%, with methane conversion of 5–10% under 30–60 bar and 450–500 °C. In liquid-phase DMTM routes, a crucial factor is the selection of a convenient solvent [22]. The major obstacle is the need for catalysts that not only exhibit adequate selectivity and reactivity, but also tolerate oxidation and protic solvents. Liquid-phase DMTM reactions generally present methane conversion limited to ≈10% [23]. The main challenge of gas-phase and liquid-phase DMTM is to preserve the formed methanol, stabilizing it to prevent further oxidation, since the reaction medium conditions are aggressive and usually promote methanol degradation.

In this context, supercritical DMTM conducted in supercritical water (SCW) emerges as an alternative to the DMTM reaction. In supercritical DMTM, the properties of the reaction medium (supercritical solvent properties) can be adjusted by manipulating the pressure and temperature [24]. Supercritical water (SCW) ($P > 22.12$ MPa, $T > 374.3$ °C) is an effective supercritical DMTM solvent since it readily dissolves the formed methanol, stabilizing it and preventing further oxidation perpetrated by the gaseous air, i.e., creating a special reaction medium [25]. Savage et al. [24] investigated DMTM-SCW's feasibility ($T = -481$ °C) and obtained methane conversion of up to 6%, oxygen conversion of up to 100% and methanol selectivity ranging from 4 to 75%. The authors noted that the highest selectivity occurred at lower conversion rates. Lee and Foster [26] investigated DMTM in supercritical water (DMTM-SCW) using an isothermal laminar reactor at 250 bar, at varying temperatures in the 400–450 °C range. The authors showed that methane was oxidized mainly to CO, CO₂ and methanol, wherein the highest methanol selectivity reached $\approx 35\%$ for 1–3% methane conversion at 400–410 °C. The authors also detected the small formation of hydrogen and attributed it to the water–gas shift reaction. Regarding the operational difficulties brought by supercritical DMTM, they are obviously the high pressure and temperature [25], but these conditions would be also encountered in the case of methanol production through the conventional NG reforming and synthesis gas conversion route [25], which, in fact, is a much more complex and expensive process. Moreover, NG production and NG processing on oil-and-gas offshore rigs are essentially characterized by high pressure (e.g., membrane skids operating at 70 bar or higher, gas lift injection lines at pressures around 200 bar or higher, CO₂ injection lines at 400 bar or higher, water injection lines above 200 bar, etc.). Thus, particularly high pressures are not a major concern on deep-water gas-and-oil offshore rigs. It is reasonable to suppose that these severe conditions of supercritical DMTM are not especially problematic in the offshore rig context. Moreover, the proposed supercritical DMTM is a once-through version with a short-residence-time reactor, to avoid methanol selectivity losses through parasitic oxidations, i.e., supercritical DMTM does not prescribe a recycle loop around the small DMTM reactor, in spite of the low methane conversion. This fact considerably simplifies the process because high-pressure recycle compressors, pumps, intercoolers, knock-out vessels, several heat exchangers and complex large reactors are eliminated. Lastly, the high pressure and high temperature investment of supercritical DMTM is somewhat recovered via power generation through adiabatic expanders after the DMTM.

1.3. The Present Work

The present work proposes supercritical DMTM insertion upstream of the GTW without DMTM recycling. The intention here is to evaluate the conversion of a part of the CO₂-rich NG into valuable methanol products before burning the rest of the NG in the GTW. The supercritical DMTM route is chosen due to its high selectivity to methanol and the non-requirement for another chemical solvent, and water is a safe and inexpensive raw material whose reposition is not necessary. Offshore DMTM-SCW coupled to GTW employing EGR, CCS and CDU configures a new processing route for CO₂-rich NG available at remote offshore locations. This new route is denoted here by DMTM-GTW-CCU. There is a clear literature gap concerning DMTM-GTW-CCU with DMTM-SCW. To fill this gap, the present work designs and investigates—via techno-economic and thermodynamic (Second Law) analyses—an innovative conceptual offshore DMTM-GTW-CCU with DMTM-SCW and explores its peculiarities.

2. Methods

Offshore DMTM-GTW-CCU fed with CO₂-rich NG exports methanol and power and dispatches CO₂-to-EOR. The DMTM-GTW-CCU system was designed and simulated in Aspen-HYSYS for technical, economic and thermodynamic evaluations. The necessary theoretical frameworks are discussed in this section.

2.1. Process Structure

Figure 1 displays a block diagram defining the DMTM-GTW-CCU sub-systems, while Table 1 depicts the simulation and design assumptions. The skeleton of the medium-capacity (≈ 450 MW) offshore DMTM-GTW-CCU comprises (i) a feed compression unit (FCU) to achieve DMTM at a supercritical water (DMTM-SCW) reactor pressure; (ii) the DMTM-SCW reactor; (iii) methanol–water separation (MWS); (iv) a light-ends combustion unit (LECU) that fires light residual hydrocarbons (methane, ethane and propane) from MWS; (v) the NGCC plant; (vi) low-pressure PCC-MEA for CO₂ capture; (vii) the first CO₂ compression unit (CU-1); (viii) CO₂ dehydration via high-pressure absorption with triethylene glycol (TEG) for water removal from the CO₂-to-EOR stream (CDU-TEG); (ix) a stripping gas unit (SGU) that adjusts the stripping gas to the CDU-TEG reboiler; (x) the second CO₂ compression unit (CU-2) that addresses CO₂-to-EOR; (xi) the EGR structure; and (xii) a primary cooling system (PCS).

Table 1. Design and simulation assumptions.

Item	Description	Assumption
A1	Thermodynamic Models	Gas, Liquid and Supercritical Streams: Peng–Robinson–Two Equation of State [27,28]; Rankine Cycle and CW: ASME Steam Table; MWS: NRTL + Peng–Robinson Equation of State (NRTL-PR); PCC-MEA: HYSYS Acid Gas Package; CDU-TEG: HYSYS Glycol Package
A2	Raw CO ₂ -Rich NG	6.5 MMSm ³ /d; T = 40 °C; P = 25 bar; CH ₄ = 49.82%mol, CO ₂ = 43.84%mol, C ₂ H ₆ = 2.99%mol, C ₃ H ₈ = 1.99%mol, iC ₄ H ₁₀ = 0.3%mol, C ₄ H ₁₀ = 0.2%mol, iC ₅ H ₁₂ = 0.2%mol, C ₅ H ₁₂ = 0.1%mol, C ₆ H ₁₄ = 0.1%mol, C ₇ H ₁₆ = 0.05%mol, C ₈ H ₁₈ = 0.03%mol, C ₉ H ₂₀ = 0.01%mol, C ₁₀ H ₂₂ = 0.01%mol, H ₂ O = 0.36%mol [2,29]
A3	Air	T = 25 °C; P = 1.013bar; N ₂ = 77.49%mol; O ₂ = 20.60%mol; H ₂ O = 1.91%mol [29]
A4	Water	T = 35 °C; P = 1.013bar; H ₂ O = 100%mol
A5	DMTM Reaction (DMTM-SCW)	T = 410 °C; P = 250 bar; DMTM-SCW Reaction Feed: CH ₄ /H ₂ O mol ratio = 1; Conversions: O ₂ = 100%; CH ₄ = 4.5% [26]; Selectivity: CO = 50%; CO ₂ = 22%; CH ₃ OH = 28% [26]
A6	Methanol–Water Separation System (MWS)	Light-Ends Column (LEC): Stages ^{Theoretical} = 20; P ^{Top} = 7 bar; T ^{Top} = 35 °C; T ^{Reboiler} = 139.6 °C; MWSC-1: Stages ^{Theoretical} = 20; P ^{Top} = 1.013 bar; T ^{Top} = 72.7 °C; T ^{Reboiler} = 100.8 °C; MWSC-2: Stages ^{Theoretical} = 20; P ^{Top} = 1.013 bar; T ^{Top} = 64.3 °C; T ^{Reboiler} = 100.8 °C; Methanol Purity: $\geq 99.85\%w/w$ (Grade AA) [30]
A7	PCC-MEA	Absorber: Stages ^{Theoretical} = 40; P ^{Top} = 1.013 bar; T ^{Inlet-Top} = 40 °C; Capture $\approx 90\%$ [29]; Stripper: Stages ^{Theoretical} = 10; P ^{Top} = 1.013 bar; T ^{Top} = 35 °C; T ^{Reboiler} = 102.6 °C [29]; Lean MEA: H ₂ O = 64.75%w/w, MEA = 30.44%w/w, CO ₂ = 4.81%w/w [29]; Capture Ratio: CR = 13.7 kg ^{Solvent} /kg ^{CO₂} ; Stripping Heat Ratio: HR = 223.5kJ/mol ^{CO₂} [29]
A8	CO ₂ Dehydration Unit (CDU-TEG)	Absorber: Stages ^{Theoretical} = 15; P = 50 bar; T ^{Inlet} = 35 °C; Lean Solvent: TEG = 98.5%w/w; Stripper: Stages ^{Theoretical} = 10; P ^{Top} = 1.013 bar; T ^{Top} = 35 °C; T ^{Reboiler} = 138.9 °C [31]
A9	Gas Turbine	Aero-Derivative Siemens SGT-A35; Efficiency ^{LHV} = 33.8% [32]; p ^{Inlet} = 25 bar; T ^{Flue-Gas} = 484 °C [32]
A10	Steam Turbine	HPS: p ^{Inlet} = 24 bar; p ^{Outlet} = 0.12 bar; T ^{Inlet} = 459 °C; Outlet Quality = 95.0%
A11	Compressors	Stage Compression Ratio ≈ 3.0 [29]; Intercoolers: T ^{Gas-Outlet} = 35 °C; $\Delta T^{\text{Approach}}$ = 5 °C; ΔP = 0.5 bar
A12	Adiabatic Efficiencies	$\eta^{\text{Pumps}} = \eta^{\text{Compressors}} = \eta^{\text{Steam-Turbine}} = 75\%$ [29]; Gas Turbines: $\eta^{\text{Air-Compressor}} = 87.3\%$, $\eta^{\text{Expander}} = 86.2\%$
A13	HRSG	$\Delta P^{\text{Flue-Gas}} = 0.025$ bar; $\Delta P^{\text{Steam}} = 0.05$ bar; $\Delta T^{\text{Approach}} = 25$ °C [33]
A14	Exchangers	$\Delta T^{\text{Approach}} = 10$ °C (gas–gas, liq–liq); $\Delta T^{\text{Approach}} = 5$ °C (gas–liq); $\Delta P = 0.5$ bar [29]
A15	Low-Pressure Steam (LPS)	T ^{LPS} = 154.6 °C; P ^{LPS} = 5.4 bar
A16	Steam Production	Priority: LPS ^{MWS} + LPS ^{PCC-MEA} + LPS ^{CDU-TEG} ; Surplus: HPS ^{Rankine-Cycle}
A17	Cooling Water (CW)	CW: T ^{Inlet} = 30 °C; T ^{Outlet} = 45 °C; p ^{Inlet} = 4 bar; p ^{Outlet} = 3.5 bar [29]
A18	Sea Water	SW: T ^{Inlet} = 25 °C (Tropical Latitudes); T ^{Outlet} = 35 °C; $\Delta P^{\text{Pump}} = 1.5$ bar
A19	CO ₂ -to-EOR	T = 35 °C; P = 300 bar; Purity: CO ₂ $\geq 99.9\%$ mol [29]

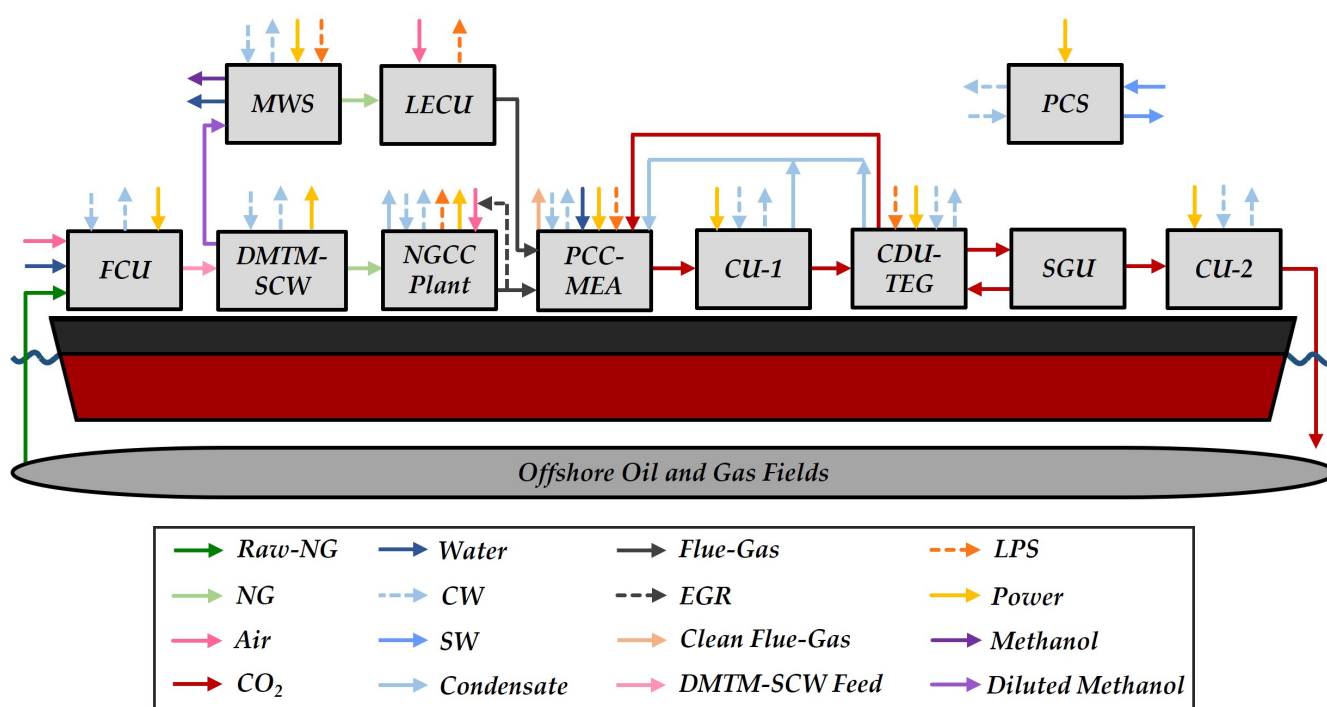


Figure 1. Process sub-systems (FCU: feed compression unit; DMTM-SCW: direct-methane-to-methanol in supercritical water; MWS: methanol–water separation system; LECU: light-ends combustion unit; NGCC: NG combined cycle; PCC-MEA: post-combustion capture with aqueous MEA; CU: CO₂ compression unit; CDU-TEG: CO₂ dehydration unit with TEG; SGU: stripping gas unit; PCS: primary cooling system; EGR: exhaust gas recycling; CW: cooling water; SW: sea water; LPS: low-pressure steam).

2.1.1. Feed Compression Unit

The supercritical DMTM step proposed in this research is an adaptation of the experiment carried out by Lee and Foster [26], which uses, in addition to water, raw CO₂-rich NG (CH₄ = 49.82%mol) and air (O₂ = 20.60%mol), as feeds, instead of pure CH₄ and O₂, respectively. The reactant streams (Figure 2) need to pass through compression trains (compressors with stage compression ratio ≈ 3 and pumps with stage compression ratio = 4) to reach the DMTM-SCW reaction pressure ($P = 250$ bar). The aqueous condensates generated by air and NG compression are mixed, according to their pressure, in the water compression train.

2.1.2. Direct Methane-to-Methanol in Supercritical Water (DMTM-SCW)

The high-pressure stream that leaves the FCU ($T = 31.4$ °C, $P = 250$ bar) is heated with the reactor product stream ($T = 410$ °C) in a plate exchanger (Plate Exch-1). To simulate the DMTM-SCW reaction in Aspen-HYSYS, an adiabatic conversion reactor was used ($O_2^{Conv} = 100\%$, $CH_4^{Conv} = 4.5\%$), considering CO, CO₂ and methanol as products and using 50%, 22% and 28% for their selectivities, respectively [26]. After the reactor (Figure 3), the cooled product stream passes through a flash separator (FI-1), where the generated gas stream is first sent to an expander (EXP), reducing its temperature and pressure ($T = 11.6$ °C, $P = 35$ bar) while generating power, and subsequently to a three-phase separator, which separates the gas, liquid hydrocarbon and aqueous phases. The FI-1 liquid stream ($T = 410$ °C, $P = 250$ bar) heats the streams leaving the three-phase separator and, after being cooled and having its pressure reduced ($T = 70.2$ °C, $P = 25$ bar), passes to another flash separator (FI-2). The FI-2 gas stream mixes with the other gas and hydrocarbon streams, forming the fuel gas that feeds the NGCC, and the FI-2 liquid stream mixes with the aqueous stream and is sent to the methanol–water separation system (MWS).

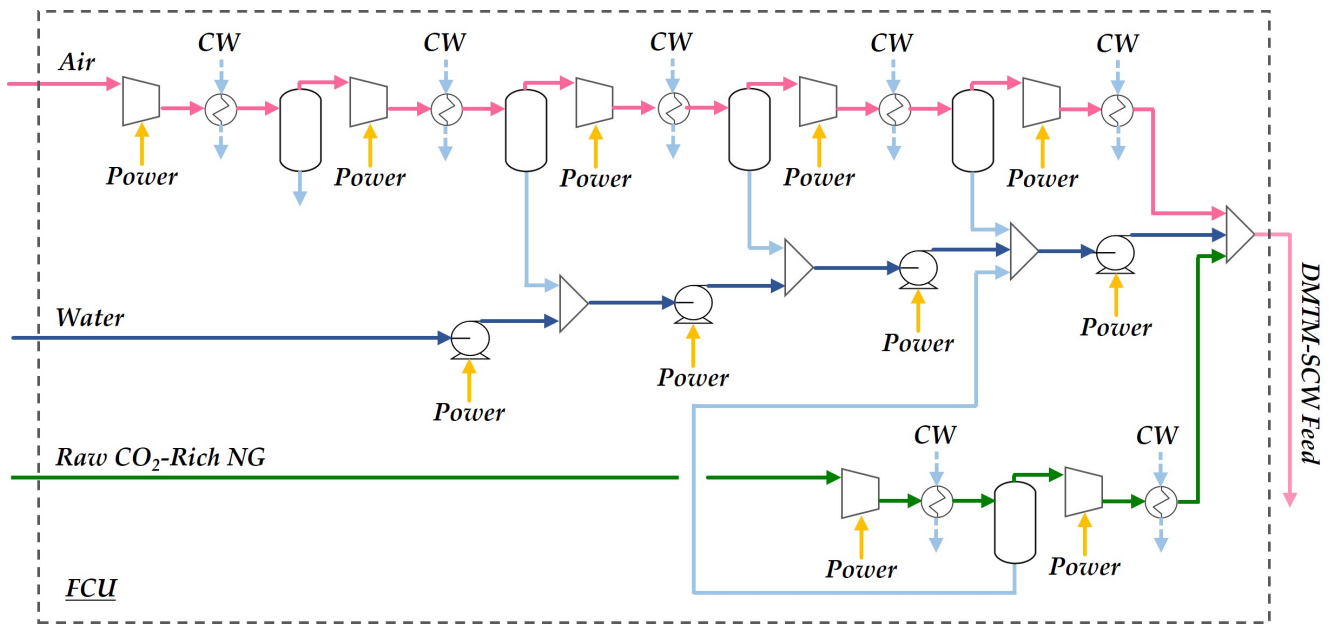


Figure 2. Feed compression unit (FCU) (DMIM-SCW: direct methane-to-methanol in supercritical water; CW: cooling water).

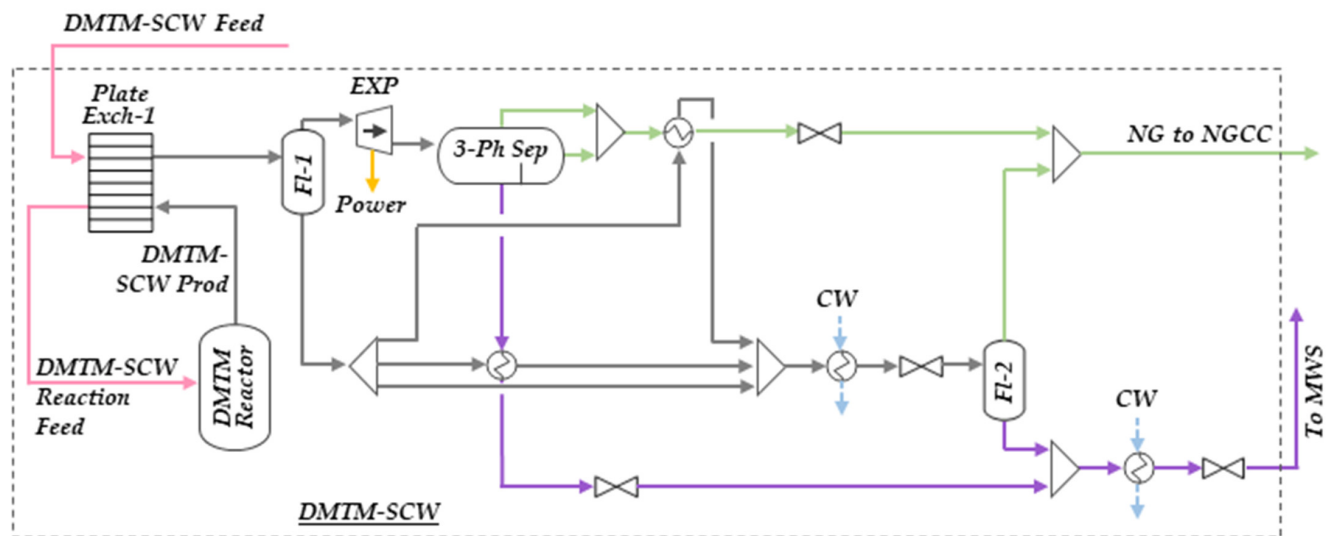


Figure 3. Direct methane-to-methanol in supercritical water (DMIM-SCW) (NGCC: natural gas combined cycle; MWS: methanol–water separation system; CW: cooling water; Exch: exchanger; Fl: flash; EXP: expander; 3-Ph Sep: 3-phase separator).

The Peng–Robinson–Two equation of state was selected in sub-systems that operate with the supercritical phase (FCU and DMIM-SCW) due to the fact that this equation of state guarantees adequate thermophysical property calculations in the supercritical region and the suitable calculation of VLE in multicomponent systems containing polar species such as water and methanol [27,28].

2.1.3. Methanol–Water Separation and Light-Ends Combustion

As shown in Figure 4, MWS is composed of three distillation columns: (i) the light-ends column (LEC), (ii) methanol–water separation column 1 (MWSC-1) and (iii) methanol–water separation column 2 (MWSC-2). The LEC is a 20-staged column ($P = 7$ bar) and aims to remove nitrogen, hydrogen, CO, CO₂ and light hydrocarbons (methane, ethane and propane) from the methanol–water mixture. The LEC top stream current ($T = 35$ °C) is sent

to the light-ends combustion chamber (LECC), generating a hot flue gas (FG) ($T = 425.6\text{ }^{\circ}\text{C}$) that produces LPS ($T^{\text{LPS}} = 154.6\text{ }^{\circ}\text{C}$, $P^{\text{LPS}} = 5.4\text{ bar}$) in the light-ends combustion exchanger (LECE). The cooled flue gas ($T = 40\text{ }^{\circ}\text{C}$) that leaves the LECE is sent to PCC-MEA. A combustion chamber is modeled as an adiabatic conversion reactor in Aspen-HYSYS.

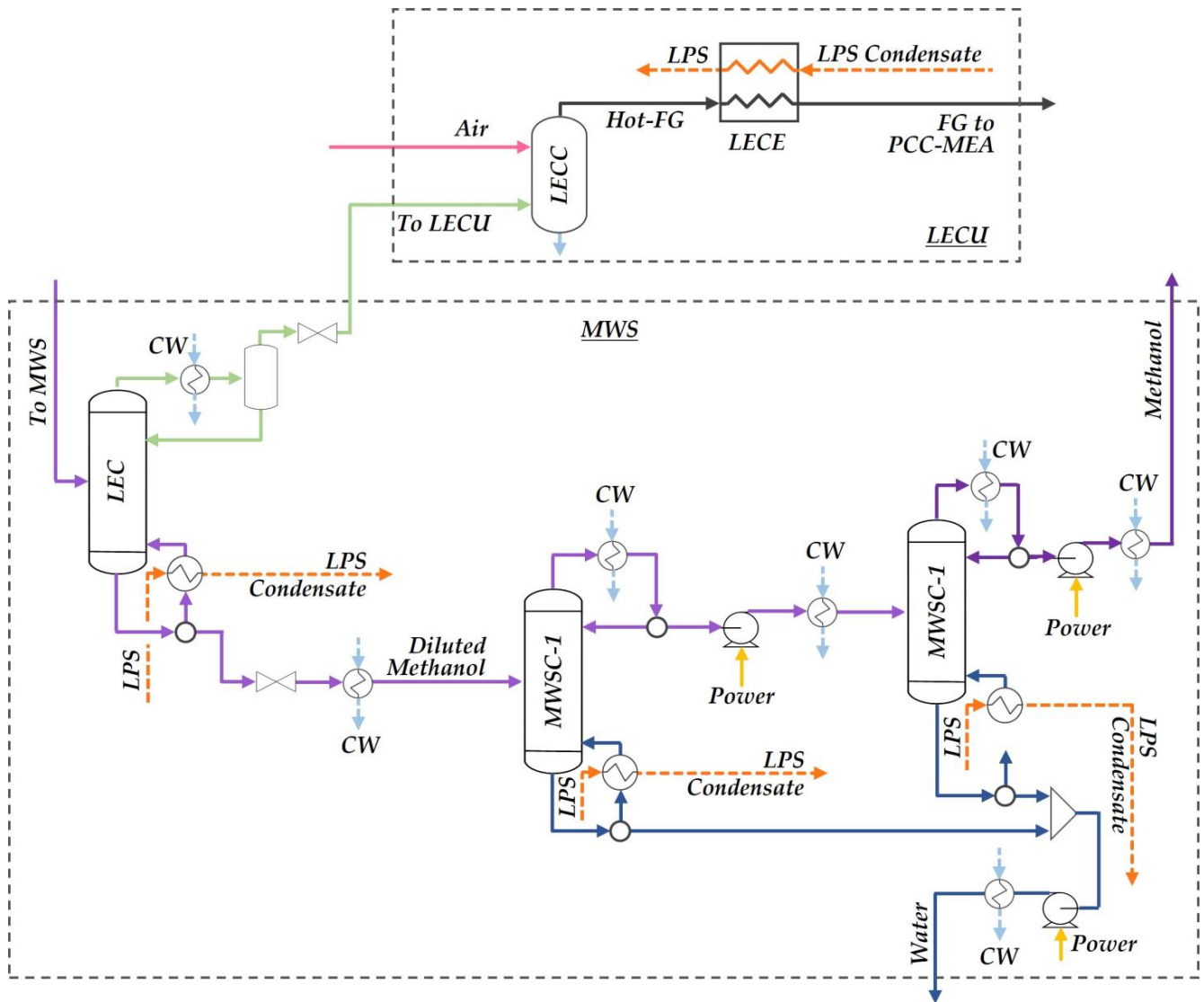


Figure 4. Methanol–water separation system (MWS) and light-ends combustion unit (LECU) (FG: flue gas; PCC-MEA: post-combustion capture with aqueous MEA; LEC: light-ends column; LECC: light-ends combustion chamber; LECE: light-ends combustion exchanger; CW: cooling water; LPS: low-pressure steam).

MWSC-1 is a 20-staged column ($P = 1.013\text{ bar}$) that receives the LEC bottom stream and aims to concentrate the methanol. The MWSC-1 top stream is directed to MWSC-2 (20 stages, $P = 1.013\text{ bar}$), which has the function of reaching Grade AA methanol purity (99.85% w/w) [30]. Pure water is produced in the MWSC-1 and MWSC-2 bottom streams. All columns require LPS ($T^{\text{LPS}} = 154.6\text{ }^{\circ}\text{C}$, $P^{\text{LPS}} = 5.4\text{ bar}$) to heat their reboilers.

2.1.4. Natural Gas Combined Cycle Plant

The NGCC plant contains four parallel NGCC elements for suitable electricity generation ($\approx 550\text{ MW}$). Each NGCC element (Figure 5) consists of four gas turbines sending hot flue gas to one heat recovery steam generator (HRSG), which heats a steam Rankine cycle. Compared with a gas turbine simple cycle, the combined cycle substantially lowers the

ratio of CO₂ emitted per MWh generated [33]. Gas turbines of the aero-derivative type (Table 1) are more appropriate in offshore rigs thanks to their lower weight-to-power [34] and footprint-to-power ratios [35], besides enhanced crew safety and simple maintainability [36]. Gas turbines directly burn raw CO₂-rich NG (CO₂ > 40%mol), producing a flue gas (FG) that feeds the HRSG at T = 484 °C [32], where low-pressure steam (LPS) (T^{LPS} = 154.6 °C, P^{LPS} = 5.4 bar) and high-pressure superheated steam (HPS) (T^{HPS} = 459 °C, P^{HPS} = 24 bar) are produced from liquid water at the respective pressures. HPS expands in the steam turbine to P = 0.12 bar and is cooled down in the sub-atmospheric condenser with cooling water (CW), recycled as a condensate to HRSG at T = 45 °C. The HRSG- and LECE-produced LPS heats the MWS, PCC-MEA and CDU-TEG reboilers. Hence, the Rankine cycle power is restrained by the LPS demand.

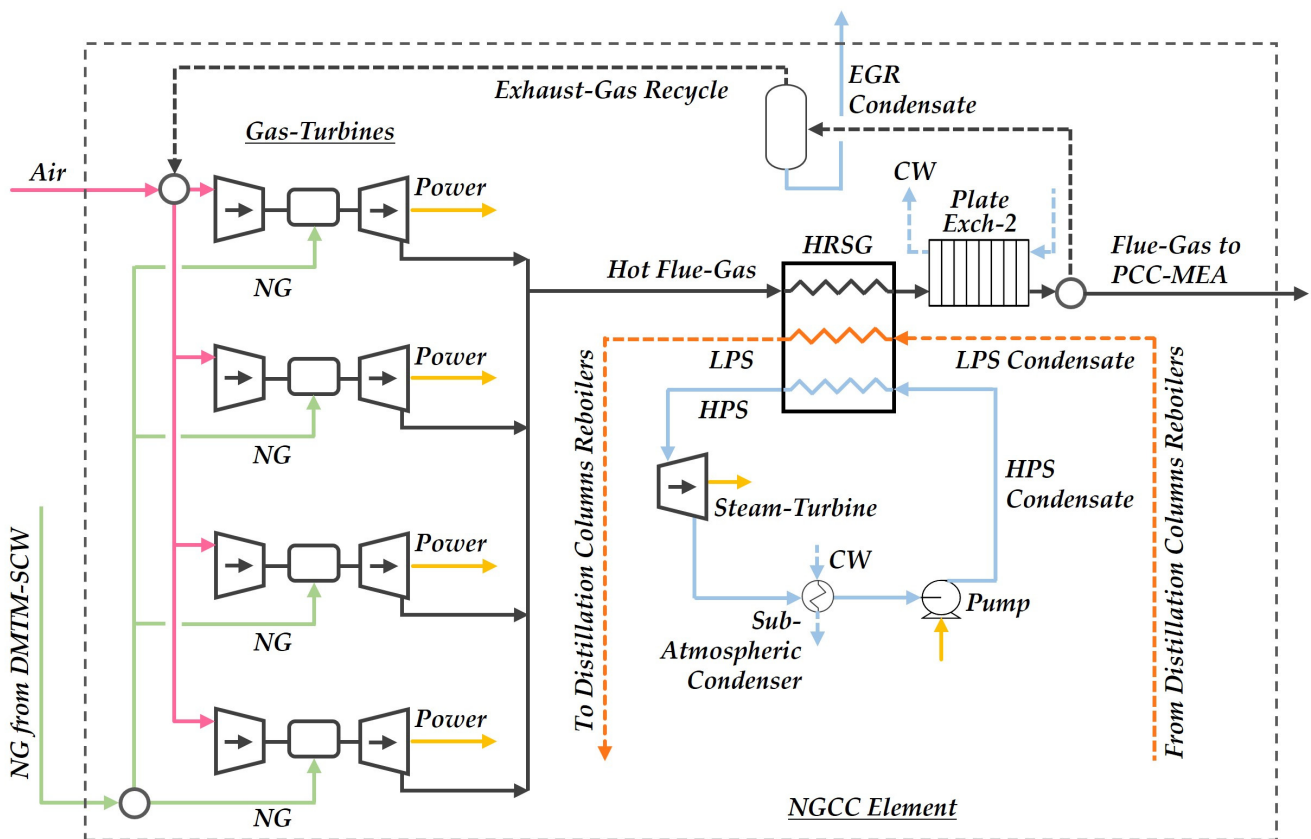


Figure 5. NG combined cycle (NGCC) element (DMTM-SCW: direct-methane-to-methanol in supercritical water; EGR: exhaust gas recycling; HRSG: heat recovery steam generator; CW: cooling water; LPS: low-pressure steam; HPS: high-pressure steam; PCC-MEA: post-combustion capture with aqueous MEA; Exch: exchanger).

The gas turbine model in Aspen-HYSYS includes (i) an adiabatic single-stage air compressor; (ii) a combustion chamber modeled as an adiabatic conversion reactor; and (iii) an adiabatic expander. This model was calibrated to factory settings by manipulating the adiabatic efficiencies of the air compressor and expander. Air is supplied at stoichiometric proportions for complete NG combustion. To limit the combustion temperature to manufactory constraints, stoichiometric air is mixed with the EGR stream. Recycled flue gas is extracted after Plate Exchanger 2 (T = 40 °C) and its flow rate is adjusted to match the recommended flue gas temperature at the expander outlet (T = 484 °C).

2.1.5. Post-Combustion Capture with Aqueous MEA

The flue gas (FG) (T = 40 °C) that leaves Plate Exchanger 2 from the four NGCC elements is connected to the flue gas (FG) from the LECE (T = 40 °C) and both are sent

to the PCC-MEA for decarbonation with aqueous MEA (MEA $\approx 30\%w/w$). The flue gas feed is distributed in the PCC-MEA absorber through four plates (Figure 6) for better overall mass transfer [37]. The PCC-MEA is designed to abate 90% of the CO₂ in the flue gas. Two parameters that define the solvent recirculation and stripper duty are critical in PCC-MEA design: (i) the capture ratio (CR—kg of fresh solvent per kg of captured CO₂) and (ii) the stripper heat ratio (HR—kJ per kg of captured CO₂). Ideal values for the CR (10–15 kg^{Solvent}/kg^{CO₂}) and HR (2000–4500 MJ/t^{CO₂}) are reported by Araújo et al. [38].

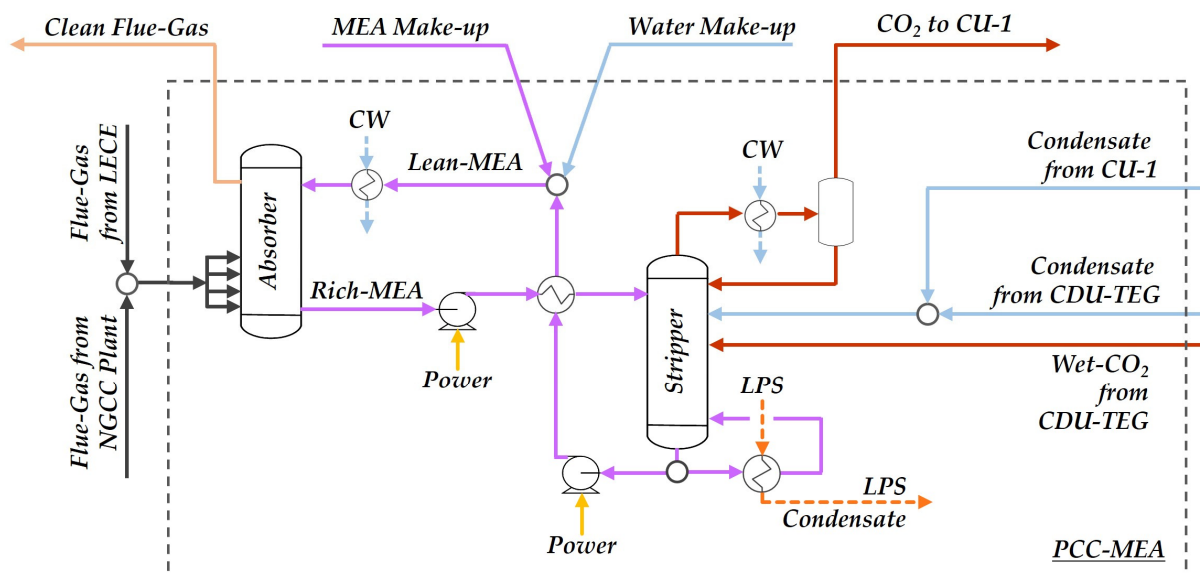


Figure 6. Post-combustion capture with aqueous MEA (PCC-MEA) (CDU-TEG: CO₂ dehydration unit with TEG; CU: CO₂ compression unit; LPS: low-pressure steam; CW: cooling water).

The atmospheric PCC-MEA stripper (Figure 6) demands LPS ($T^{\text{LPS}} = 154.6 \text{ }^\circ\text{C}$, $P^{\text{LPS}} = 5.4 \text{ bar}$) to heat the reboiler ($T = 102.6 \text{ }^\circ\text{C}$). The stripper condenser operates in total reflux (i.e., 100% condensate reflux) and releases water-saturated CO₂ ($P = 1 \text{ atm}$) through its vent. In order to keep CO₂ restricted within the CO₂ loop between the PCC-MEA and CDU-TEG units, all condensed carbonated waters ($T = 35 \text{ }^\circ\text{C}$) from the CU-1 knock-out vessels and from the TEG stripper condenser ($T = 35 \text{ }^\circ\text{C}$) are recycled to PCC-MEA stripper tray #1, while wet CO₂ from the TEG stripper condenser vent ($T = 35 \text{ }^\circ\text{C}$) is recycled to tray #10. This water recycling lowers the water make-up and condenser heat duty and avoids fugitive liberations of CO₂ from the CU-1 and CDU-TEG units. Lean MEA is recycled to the PCC-MEA absorber through a pump after the addition of water and MEA make-ups.

2.1.6. CO₂ Compression Units, CO₂ Dehydration Unit and Stripping Gas Unit

CU-1 (Figure 7a) is a four-staged intercooled compression train (stage compression ratio ≈ 3) to raise the CO₂ stream pressure up to 50 bar for CO₂ dehydration, favoring water removal [39]. The CO₂ to CDU-TEG stream ($\approx 2730 \text{ ppm-mol H}_2\text{O}$) and TEG solvent ($98.5\%w/w$ TEG) feed the 15-staged TEG absorber (Figure 7b), producing dry CO₂ ($\approx 160 \text{ ppm-mol H}_2\text{O}$) for the SGU unit as the top product and rich TEG ($\text{H}_2\text{O} \approx 55\% \text{ mol}$) as the bottom product. The TEG solvent is regenerated in the 10-staged TEG stripper, which produces lean TEG as the bottom product ($T = 138.9 \text{ }^\circ\text{C}$) and vapor wet CO₂ and carbonated liquid water as top distillate products in the partial condenser. Both the water and wet CO₂ distillates are recycled to the PCC-MEA, blocking CO₂ emissions. The SGU is a small-scale unit that adjusts the stripping gas (1.5% of dry CO₂) in order to control the TEG stripper reboiler temperature below $140 \text{ }^\circ\text{C}$ [31]. These two dry CO₂ streams feed a countercurrent heat exchanger (Figure 7c), granting a slight temperature reduction ($\approx 0.5 \text{ }^\circ\text{C}$) in the EOR-CO₂ stream. The remaining dry CO₂ is sent to CU-2 (Figure 7c) to achieve the EOR pipeline pressure ($P = 300 \text{ bar}$).

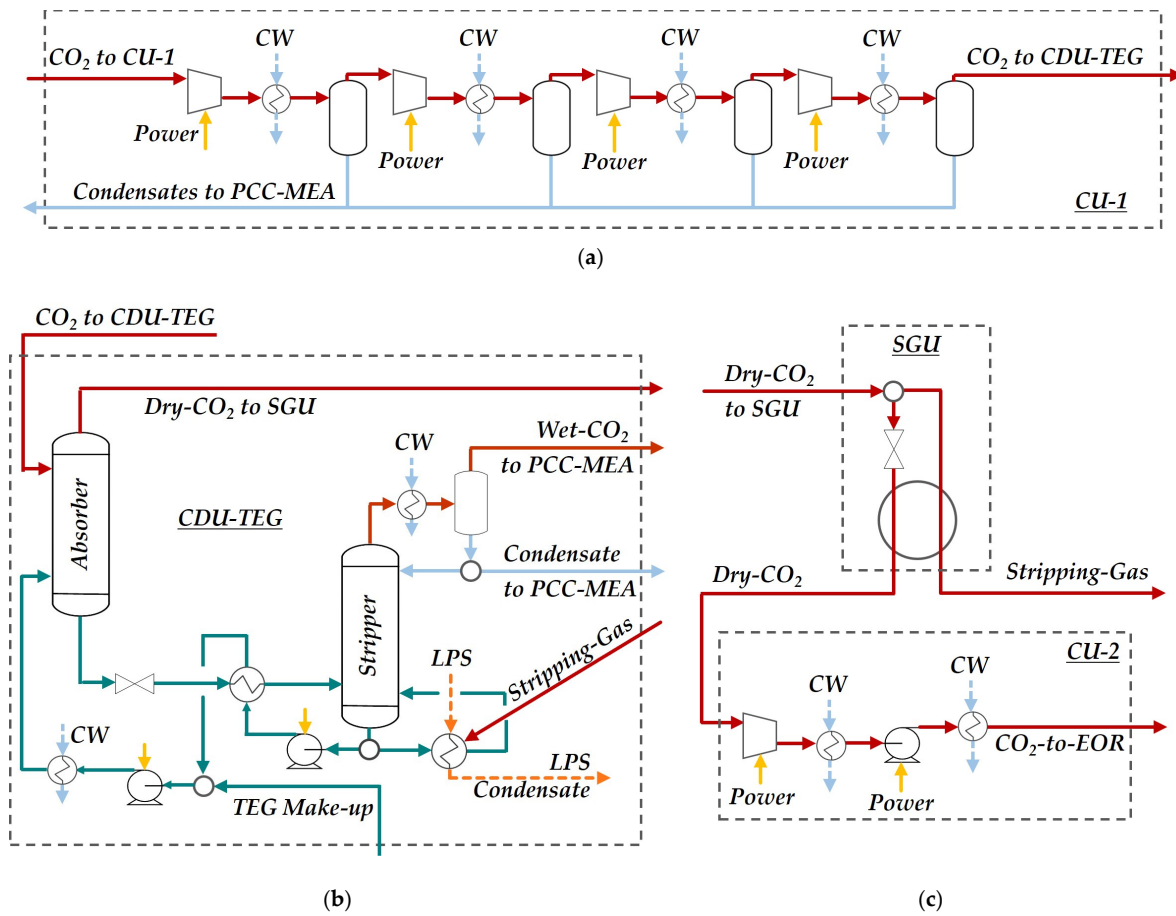


Figure 7. Compression units CU-1 (a); CU-2 (c); CO₂ dehydration unit with TEG (b) (CDU-TEG) and stripping gas unit (SGU) (c) (CW: cooling water; LPS: low-pressure steam; PCC-MEA: post-combustion capture with aqueous MEA; EOR: enhanced oil recovery).

2.1.7. Primary Cooling System

Figure 8 exhibits the primary cooling system (PCS) that regenerates cold CW (T = 30 °C) by cooling down hot CW (T = 45 °C) from the intercoolers, condensers and Plate Exchanger 2 (NGCC). Sea water (SW) is the cooling medium and it is collected from the sea surface at tropical latitudes (T = 25 °C) and returns to the sea at T = 35 °C. After this heat exchange carried out through Plate Exchanger 3, cold CW (T = 30 °C) is pumped back to be processed (P = 4 bar).

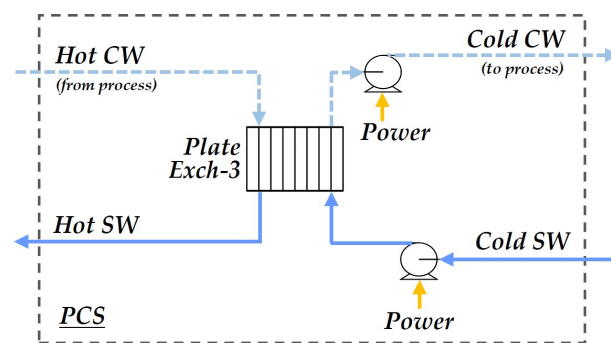


Figure 8. Primary cooling system (PCS) (Exch: exchanger; CW: cooling water; SW: sea water).

2.2. Process Economic Analysis

The economic analysis of DMTM-GTW-CCU was performed via Turton et al. [40] to calculate the (i) fixed capital investment FCI (MMUSD); (ii) cost of manufacturing COM

(MMUSD/y); (iii) revenues REV (MMUSD/y); (iv) gross annual profit GAP (MMUSD/y) and annual profit AP (MMUSD/y); and (v) net present value NPV (MMUSD). FCI (MMUSD) was estimated via Equation (1) through the bare module costs (C_{BM}) determined from the reference purchase costs, which are updated with the CEPCI Chemical Engineering Plant Cost Index (CEPCI = 816, for 2022 [41]). C_{BM} was calculated via the Six-Tenth Rule (Equation (2)) for equipment capacities above/below correlation limits using the equipment capacity (CAP) at limiting and design conditions. The data used for FCI calculation can be found in Table S1 in the Supplementary Materials file. CUT (MMUSD/y) represents the cost of utilities given by Equation (3) and COM (MMUSD/y) is calculated through Equation (4), where COL (MMUSD/y) and CRM (MMUSD/y) stand for the annual costs of labor and raw materials. GAP (MMUSD/y), AP (MMUSD/y) and NPV (MMUSD) are found via Equations (5) and (6), wherein REV (MMUSD/y), DEPR (MMUSD/y), ITR (%), i (%) and $N(y)$, respectively, represent annual revenues, annual depreciation, the income tax rate, the annual interest rate and the project lifetime (Table 2). Offshore DMTM-GTW-CCU revenues include electricity and methanol exportation, besides the increment in oil production from the EOR yield generated by CO₂ injection in the reservoir.

$$FCI = 1.18 \left(\sum_{j=1}^{NEq} C_{BM}(j) \right) \quad (1)$$

$$C_{BM} = C_{BM}^{Lim} * (CAP/CAP^{Lim})^{0.6} \quad (2)$$

$$CUT = CUT^{EE} + CUT^{LPS} + CUT^{CW} \quad (3)$$

$$COM = 0.18 * FCI + 2.73 * COL + 1.23 * (CUT + CRM) \quad (4)$$

$$GAP = REV - COM; \quad AP = \begin{cases} GAP - (GAP - DEPR) * ITR/100 & (DEPR < GAP) \\ GAP & (DEPR \geq GAP) \end{cases} \quad (5)$$

$$NPV = -FCI(0.4 + 0.6/q) + \left(\sum_{k=2}^{N+2} AP_k/q^k \right), \quad q = (1 + i/100) \quad (6)$$

Table 2. Economic assumptions.

Item	Description	Assumption
B1	Operation Lifetime	50 y
B2	Construction Time	2y (40%FCI + 60%FCI)
B3	Operation	8400 h/y
B4	i	10%
B5	DEPR (MMUSD/y)	10%FCI
B6	ITR	34%
B7	N° of Operators	30 [40]
B8	Labor Cost	89,100 USD/(y.operator) [29]
B9	CEPCI	816 (2022) [41]
B10	FCI GT (Siemens SGT-A35)	13.5 MMUSD [32]
B11	FCI Subsea HVDC Cables	1970 USD/(MW.km) [42]
B12	FCI Rig Hull	246 MMUSD [42]
B13	NG Value	2.58 USD/MMBTU [43]
B14	MEA Price	2 USD/kg [29]
B15	TEG Price	2.5 USD/kg [44]
B16	Electricity Price	0.0821 USD/kWh [43]
B17	Methanol Price	536 USD/t [44]
B18	Oil Price	80 USD/bbl [45]
B19	EOR Yield	1.5 bbl ^{Oil} /t ^{CO2} [29]

2.3. Process Thermodynamic Analysis

Thermodynamic analysis is effective to identify the degradation of resources throughout the process. The steady-state offshore DMTM-GTW-CCU and sub-systems are assessed via an analysis of processes known as the Second Law analysis or thermodynamic analysis. In the Second Law analysis, the overall system and each of its sub-systems have to be previously identified as either a power-producing system or a power-consuming system. Figure 9a displays a steady-state open system for Second Law analysis showing various feed and product streams (arrows). The open system only makes thermal contact with an infinite and isothermal heat reservoir R_0 kept at temperature T_0 . It is important to understand that any system under Second Law analysis (i.e., the overall system or its sub-systems) complies with Figure 9a and is either a power-producing system ($\dot{W} > 0$) or a power-consuming system ($\dot{W} < 0$), but only has heat interactions with R_0 via heat absorption ($\dot{Q} > 0$) or via heat rejection ($\dot{Q} < 0$). $G_n, \bar{H}_{G_n}, \bar{S}_{G_n}$, respectively, designate the molar flow rate (kmol/s), enthalpy (MJ/kmol) and entropy (MJ/kmol·K) of the n th feed stream ($n = 1..N_f$). $K_n, \bar{H}_{K_n}, \bar{S}_{K_n}$ are analogous symbols for the n th product stream ($n = 1..N_p$).

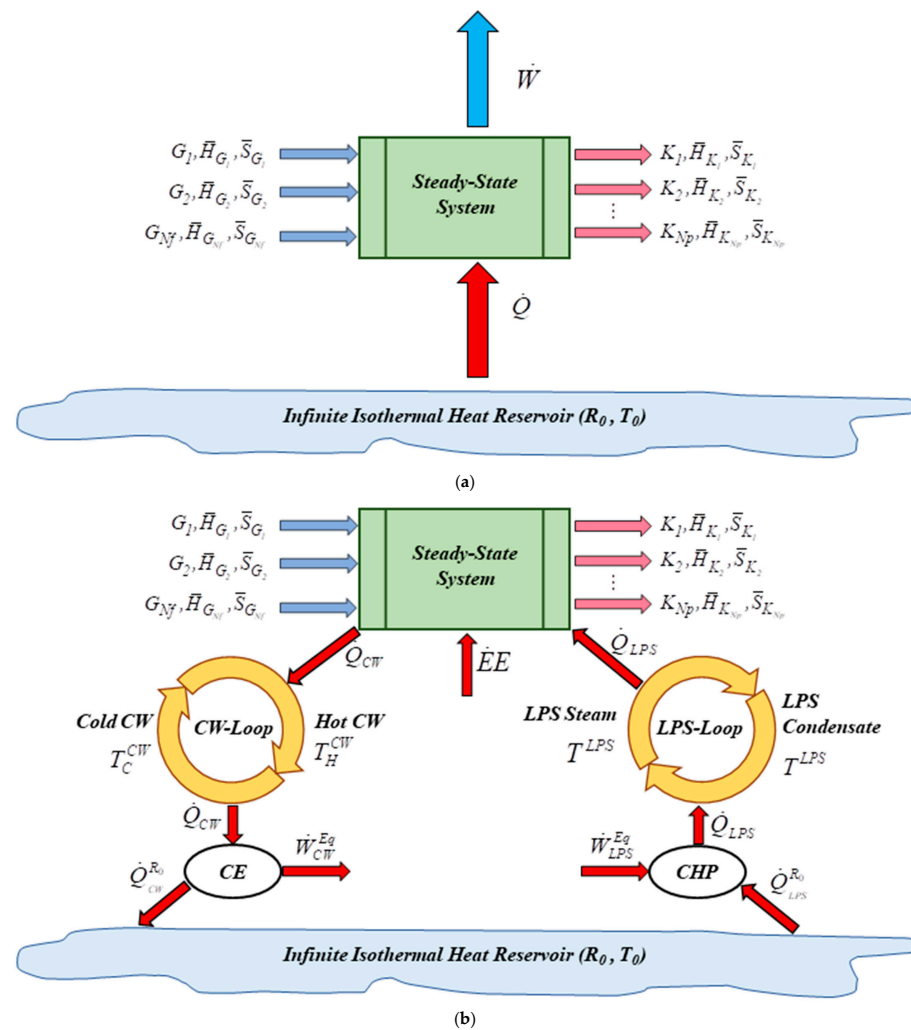


Figure 9. (a) Open system for thermodynamic analysis; (b) equivalent power for power-consuming open system (arrows as feed and product streams) that imports electricity ($\dot{E}E$), exports equivalent power via CW loop (\dot{W}_{CW}^{Eq}) and imports equivalent power via LPS loop (\dot{W}_{LPS}^{Eq}) (CW: cooling water; LPS: low-pressure steam; CHP: Carnot heat pump; CE: Carnot engine).

2.3.1. Maximum Power

Equations (7) and (8) implement the First Law of Thermodynamics for the steady-state open system depicted in Figure 9a. The system maximum power (maximum work) \dot{W}^{MAX} is calculated via the Second Law at reversibility using Equations (9)–(12). Equation (10) symbolizes the entropy balance of the Universe at reversibility, being $\dot{S}^{UNIVREV}$ the entropy creation rate of the Universe. Equation (11) is obtained from Equation (8) under reversible conditions, and Equation (12) comes from Equation (10). Finally, \dot{W}^{MAX} is calculated by means of Equation (13) or Equation (14). For power-producing systems (in general, systems performing spontaneous chemical reactions and/or spontaneous mixing or heat/mass transfers, like the DMTM-SCW, LECU, NGCC plant, SGU and PCS), Equation (14) gives a positive \dot{W}^{MAX} , while, for power-consuming systems (in general, non-spontaneous changes provided by compression/pumping systems and separation systems like the FCU, MWS, PCC-MEA, CU-1, CU-2 and CDU-TEG), a negative \dot{W}^{MAX} results.

$$\sum_{i=1}^{Nf} G_i \bar{H}_{G_i} + \dot{Q} - \dot{W} = \sum_{i=1}^{Np} K_i \bar{H}_{K_i} \quad (7)$$

$$\dot{W} = - \left(\sum_{i=1}^{Np} K_i \bar{H}_{K_i} - \sum_{i=1}^{Nf} G_i \bar{H}_{G_i} \right) + \dot{Q} \quad (8)$$

$$\dot{W} = \dot{W}^{MAX}, \quad \dot{Q} = \dot{Q}^{REV} \quad (9)$$

$$\sum_{i=1}^{Np} K_i \bar{S}_{K_i} - \sum_{i=1}^{Nf} G_i \bar{S}_{G_i} - \frac{\dot{Q}^{REV}}{T_0} = \dot{S}^{UNIVREV} = 0 \quad (10)$$

$$\dot{W}^{MAX} = - \left(\sum_{i=1}^{Np} K_i \bar{H}_{K_i} - \sum_{i=1}^{Nf} G_i \bar{H}_{G_i} \right) + \dot{Q}^{REV} \quad (11)$$

$$\dot{Q}^{REV} = T_0 \left(\sum_{i=1}^{Np} K_i \bar{S}_{K_i} - \sum_{i=1}^{Nf} G_i \bar{S}_{G_i} \right) \quad (12)$$

$$\dot{W}^{MAX} = - \left(\sum_{i=1}^{Np} K_i \bar{H}_{K_i} - \sum_{i=1}^{Nf} G_i \bar{H}_{G_i} \right) + T_0 \left(\sum_{i=1}^{Np} K_i \bar{S}_{K_i} - \sum_{i=1}^{Nf} G_i \bar{S}_{G_i} \right) \quad (13)$$

$$\dot{W}^{MAX} = - \left(\sum_{i=1}^{Np} K_i (\bar{H}_{K_i} - T_0 \bar{S}_{K_i}) - \sum_{i=1}^{Nf} G_i (\bar{H}_{G_i} - T_0 \bar{S}_{G_i}) \right) \quad (14)$$

2.3.2. Equivalent Power

Equivalent power \dot{W}^{Eq} represents the thermodynamic power equivalence of electricity production (consumption) and utility production (consumption) [29] and is always positive for regular systems. However, it can be negative for “outlaw” systems, like a theoretically power-producing system (i.e., spontaneous system) that consumes power instead of producing power (e.g., CW tower). For instance, the consumption (production) of LPS is equivalent to the consumption (production) of \dot{W}^{Eq} , while the consumption of CW is always equivalent to the production of \dot{W}^{Eq} . The offshore DMTM-GTW-CCU uses three utility types: (i) CW with flow rate J^{CW} (kmol/s), isobaric heat capacity \bar{C}_p^{CW} (MJ/kmol·K) and hot/cold temperatures T_H^{CW} (K), T_C^{CW} (K); (ii) LPS with flow rate J^{LPS} (kmol/s), vaporization enthalpy $\Delta \bar{H}_{LPS}^{VAP}$ (MJ/kmol) and temperature T^{LPS} (K); and (iii) electricity \dot{E}

(MW). \bar{C}_P^{CW} and $\Delta\bar{H}_{LPS}^{VAP}$ are assumed constant, considering that CW and LPS operate within narrow temperature ranges.

The equivalence of heat and power is settled through reversible heat engines that can attain the maximum yields of heat–work conversion. These maximum yield engines are well known as the Carnot engine (CE) and the Carnot heat pump (CHP) [29]. The CE receives heat from a hot source, generates power and discharges heat to a colder source. Analogously, the CHP absorbs power while drawing heat from a cold source and discharging heat to a hotter one. Figure 9b depicts a configuration compatible with Figure 9a, i.e., it depicts a steady-state open system thermally interacting only with the heat reservoir R_0 , generating a work effect associated with $\dot{E}E$ and other work streams. The difference is that the system in Figure 9b is a power-consuming system with the following utility effects: it absorbs $\dot{E}E$, rejects heat \dot{Q}_{CW} to the CW loop (exports power \dot{W}_{CW}^{Eq}) and absorbs heat \dot{Q}_{LPS} from the LPS loop (imports power \dot{W}_{LPS}^{Eq}). Figure 9b shows that the CW loop and LPS loop are external to the original system (but are added to it, defining a newer system compatible with Figure 9a), R_0 is always a cold heat reservoir (cold source), and \dot{W}_{CW}^{Eq} , \dot{Q}_{CW} , \dot{W}_{LPS}^{Eq} , \dot{Q}_{LPS} are always positive. It is not difficult to create an analogous version of Figure 9b for a power-producing system (i.e., in which CW is imported and electricity and LPS are exported).

The steady-state power-consuming system (Figure 9b) rejects heat (\dot{Q}_{CW}) to cold CW, producing hot CW, which is restored to cold CW via a CW loop using the CE that exports power (\dot{W}_{CW}^{Eq}) and rejects heat (\dot{Q}_{CW}) to R_0 . Equivalently, the power-consuming system absorbs heat (\dot{Q}_{LPS}) from LPS, becoming an LPS condensate, which is restored to LPS via an LPS loop, using the CHP that imports power (\dot{W}_{LPS}^{Eq}) and absorbs heat ($\dot{Q}_{LPS}^{R_0}$) from R_0 . \dot{W}_{CW}^{Eq} is obtained by Equation (16) using Equation (15a), Equation (15b) and CE entropy conservation in Equation (15c). Appropriately, \dot{W}_{LPS}^{Eq} is obtained by Equation (18) using Equation (17a), Equation (17b) and CHP entropy conservation in Equation (17c). Equation (18) also works for \dot{W}_{LPS}^{Eq} in power-producing systems, but with the difference that the LPS loop now spins counter-clockwise, the CE replaces the CHP, and all effects are reversed.

Equation (19a) calculates the equivalent power produced by a power-producing system that exports $\dot{E}E$ and LPS (counter-clockwise LPS loop in Figure 9b) and consumes CW. Analogously, Equation (19b) is the equivalent power consumed by a power-consuming system that consumes $\dot{E}E$, CW and LPS. The substitution of Equations (16) and (18) into Equation (19a,b) creates Equation (20a,b), respectively, leading to the equivalent power produced by a power-producing system and the equivalent power consumed by a power-consuming system, respectively.

$$\dot{W}_{CW}^{Eq} = \dot{Q}_{CW} - \dot{Q}_{CW}^{R_0} \quad (15a)$$

$$\dot{Q}_{CW} = J^{CW} \bar{C}_P^{CW} (T_H^{CW} - T_C^{CW}) \quad (15b)$$

$$\frac{\dot{Q}_{CW}^{R_0}}{T_0} + J^{CW} \bar{C}_P^{CW} \ln\left(\frac{T_C^{CW}}{T_H^{CW}}\right) = 0 \quad (15c)$$

$$\dot{W}_{CW}^{Eq} = J^{CW} \bar{C}_P^{CW} \left(T_H^{CW} - T_C^{CW} - T_0 \cdot \ln\left(\frac{T_H^{CW}}{T_C^{CW}}\right) \right) \quad (16)$$

$$\dot{W}_{LPS}^{Eq} = \dot{Q}_{LPS} - \dot{Q}_{LPS}^{R_0} \quad (17a)$$

$$\dot{Q}_{LPS} = J^{LPS} \Delta \bar{H}_{LPS}^{VAP} \quad (17b)$$

$$-\frac{\dot{Q}_{LPS}^{R_0}}{T_0} + J^{LPS} \frac{\Delta \bar{H}_{LPS}^{VAP}}{T_{LPS}} = 0, \quad (17c)$$

$$\dot{W}_{LPS}^{Eq} = J^{LPS} \Delta \bar{H}_{LPS}^{VAP} \left(1 - \frac{T_0}{T_{LPS}} \right) \quad (18)$$

$$\dot{W}^{Eq} = \dot{E}E + \dot{W}_{CW}^{Eq} + \dot{W}_{LPS}^{Eq} \{Power-Producing System\} \quad (19a)$$

$$\dot{W}^{Eq} = \dot{E}E - \dot{W}_{CW}^{Eq} + \dot{W}_{LPS}^{Eq} \{Power-Consuming System\} \quad (19b)$$

$$\dot{W}^{Eq} = \dot{E}E + J^{CW} \bar{C} p^{CW} \left(T_H^{CW} - T_C^{CW} - T_0 \cdot \ln \left(\frac{T_H^{CW}}{T_C^{CW}} \right) \right) + J^{LPS} \Delta \bar{H}_{LPS}^{VAP} \left(1 - \frac{T_0}{T_{LPS}} \right) \quad (20a)$$

$$\dot{W}^{Eq} = \dot{E}E - J^{CW} \bar{C} p^{CW} \left(T_H^{CW} - T_C^{CW} - T_0 \cdot \ln \left(\frac{T_H^{CW}}{T_C^{CW}} \right) \right) + J^{LPS} \Delta \bar{H}_{LPS}^{VAP} \left(1 - \frac{T_0}{T_{LPS}} \right) \quad (20b)$$

2.3.3. Thermodynamic Efficiency

Second Law analysis allows the calculation of the thermodynamic efficiency and the lost work (lost power) of the overall system and also of its sub-systems. This corresponds to estimating the degree of resource degradation in the system and its sub-systems. With \dot{W}^{MAX} (Equation (14)) and \dot{W}^{Eq} (Equation (20a,b)), the thermodynamic efficiencies of power-producing systems and power-consuming systems are calculated via Equation (21a,b), respectively.

$$\eta\% = 100 \cdot \dot{W}^{Eq} / \dot{W}^{MAX} \{Power-Producing System\} \quad (21a)$$

$$\eta\% = 100 \cdot (-\dot{W}^{MAX}) / \dot{W}^{Eq} \{Power-Consuming System\} \quad (21b)$$

2.3.4. Lost Work

Equation (22a,b) are intuitive formulas for the lost work (lost power) of power-producing systems and power-consuming systems, respectively. An alternative way to calculate lost work can be derived from the Second Law formula in Equation (23a) that represents all Universe changes resulting from system transitions, where \dot{S}^{UNIV} is the entropy creation rate of the Universe owing to the system operation. Hence, Equation (23b,c) are the lost work formulas generated by Equation (23a) for power-producing systems and power-consuming systems, respectively, where \dot{S}^{R_0} is replaced by Equation (24a,b), again, for power-producing systems and power-consuming systems.

$$\dot{W}^{LOST} = \dot{W}^{MAX} - \dot{W}^{Eq} \{Power-Producing System\} \quad (22a)$$

$$\dot{W}^{LOST} = \dot{W}^{Eq} - (-)\dot{W}^{MAX} \{Power-Consuming System\} \quad (22b)$$

$$\dot{W}^{LOST} = T_0 \dot{S}^{UNIV} = T_0 \left(\dot{S}^{R_0} + \sum_{i=1}^{Np} K_i \bar{S}_{K_i} - \sum_{i=1}^{Nf} G_i \bar{S}_{G_i} \right) \quad (23a)$$

$$\dot{W}^{LOST} = J^{CW} \bar{C}_p^{CW} T_0 \ln \left(\frac{T_H^{CW}}{T_C^{CW}} \right) + J^{LPS} \Delta \bar{H}_{LPS}^{VAP} \left(\frac{T_0}{T^{LPS}} \right) + T_0 \left(\sum_{i=1}^{Np} K_i \bar{S}_{K_i} - \sum_{i=1}^{Nf} G_i \bar{S}_{G_i} \right) \quad (23b)$$

$$\dot{W}^{LOST} = J^{CW} \bar{C}_p^{CW} T_0 \ln \left(\frac{T_H^{CW}}{T_C^{CW}} \right) - J^{LPS} \Delta \bar{H}_{LPS}^{VAP} \left(\frac{T_0}{T^{LPS}} \right) + T_0 \left(\sum_{i=1}^{Np} K_i \bar{S}_{K_i} - \sum_{i=1}^{Nf} G_i \bar{S}_{G_i} \right) \quad (23c)$$

$$\dot{S}^{R_0} = \frac{\dot{Q}_{CW}^{R_0}}{T_0} + \frac{\dot{Q}_{LPS}^{R_0}}{T_0} = J^{CW} \bar{C}_p^{CW} \ln \left(\frac{T_H^{CW}}{T_C^{CW}} \right) + J^{LPS} \frac{\Delta \bar{H}_{LPS}^{VAP}}{T^{LPS}} \quad (24a)$$

$$\dot{S}^{R_0} = \frac{\dot{Q}_{CW}^{R_0}}{T_0} - \frac{\dot{Q}_{LPS}^{R_0}}{T_0} = J^{CW} \bar{C}_p^{CW} \ln \left(\frac{T_H^{CW}}{T_C^{CW}} \right) - J^{LPS} \frac{\Delta \bar{H}_{LPS}^{VAP}}{T^{LPS}} \quad (24b)$$

3. Results and Discussion

The results from the technical, economic and thermodynamic analyses of the offshore DMTM-GTW-CCU are next presented and discussed.

3.1. Technical and Economic Performance

Table 3 summarizes the technical and economic results of the offshore DMTM-GTW-CCU. The DMTM plant, which encompasses the FCU, DMTM-SCW, MWS and LECU sub-systems, produces methanol (2.2 t/h) from methane (91.7 t/h, contained in 342.4 t/h of raw CO₂-rich NG). Grade AA methanol purity (99.85% w/w) [30] is achieved through two distillation columns: (i) MWSC-1, which aims to concentrate the methanol stream (from 1.1 to 49.0% mol), and (ii) MWSC-2, which obtains methanol specification. Pure water was generated as MWSC-1 and MWSC-2 bottom products.

Table 3. Techno-economic results.

DMTM-GTW-CCU		System	Utilities Demand		
			CW (t/h)	LPS (t/h)	Power (MW)
Gross Power (MW)	564.5	FCU	3052.5	-	35.34
Power Demand (MW)	107.4	DMTM-SCW	32.4	-	-
Net Power (MW)	457.1	MWS	2511.7	68.1	0.002
Methanol Production (t/h)	2.2	LECU	-	-	-
CO ₂ Flue Gas (t/h) (PCC-MEA Feed)	554.3	NGCC Plant	24,175.7	-	0.04
CO ₂ Emissions (t/h) (Atmosphere)	63.0	PCC-MEA	32,445.0	1189.0	0.35
CO ₂ Injected (t/h) (EOR)	491.3	CU-1	3976.6	-	50.46
		CDU-TEG	40.3	1.9	0.01
		SGU	-	-	-
		CU-2	2304.0	-	12.84
		PCS	-	-	8.32
		Total	68,538.2	1259.0	107.4
		CDU-TEG Results	Economic Results		
PCC-MEA Results		CO ₂ Inlet (ppm-mol H ₂ O)	2731.7	FCI (MMUSD)	1544.4
Flue Gas Feed (%molCO ₂)	16.7	CO ₂ Outlet (ppm-mol H ₂ O)	158.1	COL (MMUSD/y)	2.7
Clean Flue Gas (%molCO ₂)	2.1	Capture-Ratio (kg ^{TEG} /kg ^{H₂O})	5.7	CUT (MMUSD/y)	0 *
CO ₂ to CU-1 (%molCO ₂)	92.6	Lean-Solvent (t/h)	3.3	CRM (MMUSD/y)	135.5
Capture Ratio (kg ^{Solvent} /kg ^{CO₂})	13.7	Absorber: T ^{Top} (°C)/T ^{Bottom} (°C)	36.5/35.6	REV (MMUSD/y)	820.0
CO ₂ Captured (tCO ₂ /h)	492.3	Stripper: T ^{Feed} (°C)/T ^{Top} (°C)/T ^{Bottom} (°C)	78/35/139	NPV ^{50years} (MMUSD)	1020.9
Lean Solvent (t/h)	6740.0	Reboiler Duty (MW)	1.1	Payback (y)	10
Absorber: T ^{Top} (°C)/T ^{Bottom} (°C)	61.8/61.2				
Stripper: T ^{Feed} (°C)/T ^{Top} (°C)/T ^{Bottom} (°C)	83/35/103				
Heat Ratio (kJ/molCO ₂)	224				
Reboiler Duty (MW)	694				

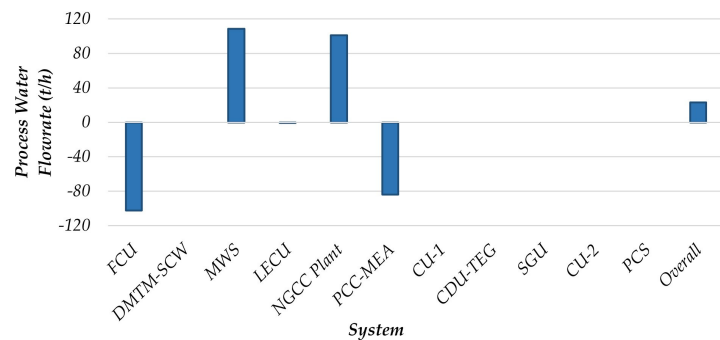
* Plant is self-sufficient in terms of electricity, CW and LPS.

The NGCC plant (with four parallel NGCC elements) of the offshore DMTM-GTW-CCU produces 564.5 MW of gross power ($\approx 97.8\%$ from gas turbines), allowing 457.1 MW of net exported power. Each gas turbine burns ≈ 23.4 t/h of fuel-gas and produces ≈ 34 MW at 33.8% LHV efficiency. EGR entails that a single NGCC element produces 1890.7 t/h flue gas at 16.7% mol CO_2 . The HRSG cools down the gas turbine flue gas from 484 °C to 160 °C, the minimum temperature for maximum HPS generation, ensuring sufficient LPS to heat the MWS, PCC-MEA and CDU-TEG reboilers.

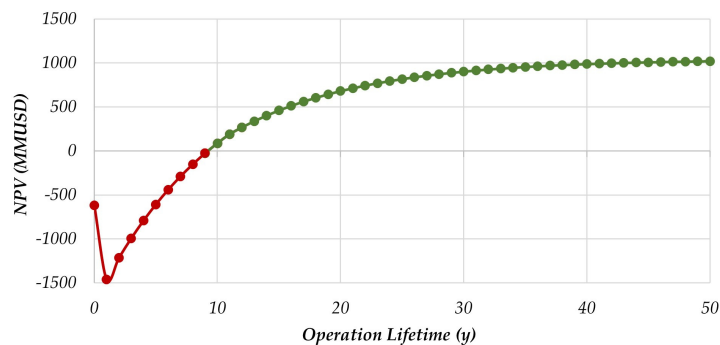
The PCC-MEA stripper requires 694.5 MW of LPS and discharges 515.0 t/h of water-saturated CO_2 as the top product. CU-1 pressurizes the CO_2 stream up to 50 bar to reach the CDU-TEG's ideal conditions for CO_2 dehydration. The CDU-TEG removes $\approx 94\%$ of the water from its feed and produces 498.4 t/h of dry CO_2 (≈ 160 ppm-mol H_2O). The SGU sends 7.1 t/h of low-pressure dry CO_2 to the TEG stripper reboiler to maintain its temperature below 140 °C to avoid TEG degradation [31]. Considering the small flow rate of the water removed from the CO_2 stream, the TEG stripper reboiler demands 1.1 MW of LPS. CU-2 exports 491.3 t/h of dry CO_2 ($P = 300$ bar, $T = 35$ °C) to EOR, avoiding the emission of this CO_2 to the atmosphere. Thus, EOR is classified as a carbon capture and utilization (CCU) process, since it produces oil from the injected CO_2 (EOR yield = 1.5 $\text{bbl}^{\text{Oil}}/\text{t}^{\text{CO}_2}$ [29]) and consequently monetizes it.

The offshore DMTM-GTW-CCU power demand corresponds to 19.0% of its gross power. The FCU, CU-1 and CU-2 are the main electricity consumers (considering their compressor trains), while the PCC-MEA leads the CW and LPS consumption.

Figure 10a shows the process of water generation or consumption of the overall system and its sub-systems. As the offshore DMTM-GTW-CCU produces water, it becomes self-sufficient in terms of this resource. Thus, it is not necessary to import water.



(a)



(b)

Figure 10. Techno-economic results: (a) process water production (+) or consumption (-) and (b) NPV (FCU: feed compression unit; DMTM-SCW: direct-methane-to-methanol in supercritical water; MWS: methanol–water separation system; LECU: light-ends combustion unit; NGCC: NG combined cycle; PCC-MEA: post-combustion capture with aqueous MEA; CU: CO_2 compression unit; CDU-TEG: CO_2 dehydration unit with TEG; SGU: stripping gas unit; PCS: primary cooling system).

The calculated economic variables (FCI, COL, CUT, CRM, REV, NPV) are presented in Table 3. One can note that the cost of utilities (CUT) is zero, since the power, LPS and CW are produced on site. Although DMTM-GTW-CCU plant implementation requires a high fixed capital investment (FCI = 1544.4 MMUSD), the project is economically feasible, considering the scenario described in Table 2. Figure 10b shows the NPV for a 50 year horizon, highlighting a payback time of 10 years.

3.2. Thermodynamic Analysis Results

Thermodynamic and lost work analyses were executed for the offshore DMTM-GTW-CCU overall system and its sub-systems, i.e., the (i) FCU; (ii) DMTM-SCW; (iii) MWS; (iv) LECU; (v) NGCC plant; (vi) PCC-MEA; (vii) CU-1; (viii) CDU-TEG; (ix) SGU; (x) CU-2; (xi) EGR structure; and (xii) PCS. The DMTM-GTW-CCU was correctly partitioned among the previously cited sub-systems (there was no sub-system missed), meaning that the respective sums of \dot{W}^{MAX} , \dot{W}^{Eq} and \dot{W}^{LOST} for all sub-systems must provide the same values as for the overall system, which are determined independently of the sub-systems. The paralleling of the overall system values with the respective sum over the sub-systems leads to a consistency check of the thermodynamic investigation. There is always some divergence between the sums over the sub-systems and the overall system in practice. Therefore, divergences below 1% could be established to confirm consistency in the thermodynamic analysis.

3.2.1. Performance of Maximum Power, Equivalent Power and Thermodynamic Efficiency

Table 4 depicts the thermodynamic efficiencies and other results of the Second Law analysis of the overall offshore DMTM-GTW-CCU and its sub-systems. The DMTM-SCW, LECU, NGCC, SGU, PCS and the overall system are power-producing systems ($\dot{W}^{MAX} > 0$); therefore, Equations (19a), (20a), (21a), (22a), (23b) and (24a) were adopted for the \dot{W}^{Eq} , $\eta\%$, \dot{W}^{LOST} calculations. Meanwhile, the FCU, MWS, PCC-MEA, CU-1, CDU-TEG and CU-2 sub-systems are power-consuming systems ($\dot{W}^{MAX} < 0$), requiring Equations (19b), (20b), (21b), (22b), (23c) and (24b) for the \dot{W}^{Eq} , $\eta\%$, \dot{W}^{LOST} calculations. The thermodynamic efficiency of the overall offshore DMTM-GTW-CCU reached 27.99% (Table 4).

Table 4. Second Law analysis and lost work validation.

System	Second Law Analysis						Lost Work Validation		
	\dot{W}^{MAX} (MW)	$\dot{E}E$ (MW)	\dot{W}_{CW}^{Eq} (MW)	\dot{W}_{LPS}^{Eq} (MW)	\dot{W}^{Eq} (MW)	$\eta\%$	\dot{W}^{LOST} (MW) *	\dot{W}^{LOST} (MW) #	Divergence (%)
FCU	−16.45	35.34	2.13	-	33.21	49.54	16.76	16.79	−0.20
DMTM-SCW	47.34	11.60	0.02	-	11.62	24.55	35.72	35.71	0.02
MWS	−0.01	0.002	1.75	12.05	10.30	0.12	10.29	10.35	−0.62
LECU	0.22	-	-	0.04	0.04	16.79	0.1819	0.1818	0.04
NGCC Plant	1686.34	552.82	16.87	222.58	792.27	46.98	894.07	893.49	0.06
PCC-MEA	−28.23	0.35	22.64	210.24	187.95	15.02	159.72	158.98	0.46
CU-1	−28.19	50.46	2.78	-	47.69	59.12	19.49	19.54	−0.23
CDU-TEG	−0.003	0.01	0.03	0.33	0.31	1.11	0.307	0.309	−0.37
SGU	0.40	-	-	-	0.00	0.00	0.40	0.40	0.00
CU-2	−4.82	12.84	1.61	-	11.23	42.95	6.41	6.43	−0.40
PCS	23.99	−8.32	-	-	−8.32	−34.69	32.31	32.49	−0.53
Sum Crosscheck							1175.66	1174.67	0.08
Overall	1633.07	457.09	-	-	457.09	27.99	1175.98	1181.54	−0.47

* via Equation (22a,b); # via Equation (23b,c).

The DMTM-SCW is a sub-system driven by spontaneities, i.e., it is a power-producing system ($\dot{W}^{MAX} = 47.34$ MW). The DMTM-SCW \dot{W}^{Eq} production (11.62 MW) is calculated with the $\dot{E}E$ produced by the expander (EXP), added to the \dot{W}_{CW}^{Eq} exported as hot CW from

two cooling water heat exchangers. There is no LPS production or consumption ($\dot{W}_{LPS}^{Eq} = 0$). The DMTM-SCW's thermodynamic efficiency reached 24.55%.

The LECU is also a power-producing system ($\dot{W}^{MAX} = 0.22$ MW). The \dot{W}^{Eq} produced (0.04 MW) comes from LPS exportation (\dot{W}_{LPS}^{Eq}). The LECU's thermodynamic efficiency was 16.79%.

With a highly positive $\dot{W}^{MAX} = 1686.34$ MW, the NGCC plant is incontestably a power-producing system as a result of its extremely spontaneous combustion transformations in the NGCC elements. The \dot{W}^{Eq} generated by each NGCC element is calculated as follows: the \dot{W}_{LPS}^{Eq} from HRSG LPS exportation is added to the \dot{W}_{CW}^{Eq} produced by the Rankine cycle condenser and added to the $\dot{E}E$ that is generated in the gas turbines and in the steam turbine minus the Rankine cycle pump power (Figure 5). The thermodynamic efficiency of the NGCC plant reached 46.98%.

As with any separation process, the MWS is a power-consuming system. As predicted, the MWS \dot{W}^{MAX} is negative (−0.01 MW), due to the equivalent power required for methanol and water separation. The MWS imported \dot{W}^{Eq} (10.30 MW) is measured as the \dot{W}_{LPS}^{Eq} consumed in the LEC, MWSC-1 and MWSC-2 reboilers, minus the \dot{W}_{CW}^{Eq} produced as hot CW from the LEC, MWSC-1 and MWSC-2 condensers and from four cooling water heat exchangers, added to the $\dot{E}E$ demanded in three pumps. The MWS' thermodynamic efficiency reached 0.12%.

As with any separation process, the PCC-MEA is a power-consuming system ($\dot{W}^{MAX} = -28.23$ MW) due to the equivalent power demanded for CO₂ separation from flue gas. The PCC-MEA \dot{W}^{Eq} consumed (187.95 MW) is obtained as follows: the \dot{W}_{LPS}^{Eq} imported by the PCC-MEA stripper reboiler, minus the \dot{W}_{CW}^{Eq} exported as hot CW from the stripper condenser and from the lean MEA cooler, added to the $\dot{E}E$ required by the solvent recirculation pump and water and MEA make-up pumps. The PCC-MEA's thermodynamic efficiency was 15.02%.

CDU-TEG is also a separation process, so it should be a power-consuming system ($\dot{W}^{MAX} = -0.003$ MW). The slight \dot{W}^{MAX} value is a result of the very low flow rate of the water removed from the CO₂ stream (≈ 2730 ppm-mol H₂O to ≈ 160 ppm-mol H₂O). The CDU-TEG \dot{W}^{Eq} (0.31 MW) imported is calculated as follows: the \dot{W}_{LPS}^{Eq} consumed in the CDU-TEG stripper reboiler, subtracted from the \dot{W}_{CW}^{Eq} produced through hot CW from the stripper condenser and from the lean TEG cooler, added to the $\dot{E}E$ demanded in the TEG recirculation pump and in the TEG make-up pump. The CDU-TEG thermodynamic efficiency reached 1.11%.

The SGU is another sub-system driven by spontaneities, being a power-producing system ($\dot{W}^{MAX} = 0.40$ MW). However, since \dot{W}_{LPS}^{Eq} , \dot{W}_{CW}^{Eq} and $\dot{E}E$ are all zero, the SGU's thermodynamic efficiency is 0%, meaning that the SGU has sufficient spontaneity to produce power, but this potential is wasted and no power is actually produced.

The FCU, CU-1 and CU-2 perform non-spontaneous (compression) changes. Therefore, they are undeniably power-consuming systems ($\dot{W}^{MAX} = -16.45$ MW, $\dot{W}^{MAX} = -28.19$ MW and $\dot{W}^{MAX} = -4.82$ MW, respectively). The respective \dot{W}^{Eq} is measured as follows: the $\dot{E}E$ imported in the compressors and pumps, minus the \dot{W}_{CW}^{Eq} produced as hot CW from the compressor intercoolers. There is no LPS consumption ($\dot{W}_{LPS}^{Eq} = 0$). The FCU, CU-1 and CU-2's thermodynamic efficiencies were, respectively, 49.54%, 59.12% and 42.95%.

The PCS is a power-producing system ($\dot{W}^{MAX} = 23.99$ MW) since it performs spontaneous changes. Nevertheless, the PCS actually consumes $\dot{E}E$ in the CW/SW pumps, i.e.,

$\dot{E}E$ contributes negatively to \dot{W}^{Eq} . It is worth highlighting that CW is a process stream in the PCS, so it should not be counted as a CW utility (i.e., $\dot{W}_{CW}^{Eq} = 0$). Moreover, the PCS does not produce LPS ($\dot{W}_{LPS}^{Eq} = 0$). Hence, the PCS has negative thermodynamic efficiency (−34.69%).

3.2.2. Lost Work Performance

Lost work corresponds to the power potential wasted in the DMTM-GTW-CCU and its sub-systems from irreversible (spontaneous) effects. Table 4 depicts the lost work results and also verifies the consistency of the present thermodynamic analysis via a comparison of the lost work values estimated through two thermodynamically independent methods, namely (i) via \dot{W}^{MAX} and \dot{W}^{Eq} in Equation (22a,b) and (ii) via $T_0 \cdot \dot{S}^{UNIV}$ in Equation (23b,c), for power-producing and power-consuming systems, respectively. In addition, Table 4 also illustrates a consistency crosscheck regarding the sum of lost work over the sub-systems, which, in theory, should equal the lost work of the overall system (numerical divergences were all smaller than 1%).

Figure 11 presents Sankey diagrams for the \dot{W}^{MAX} , \dot{W}^{Eq} and \dot{W}^{LOST} flows for the overall system and its sub-systems. In Figure 11, \dot{W}^{LOST} corresponds to the sum of lost work over all sub-systems (light maroon flows), while $\Delta\dot{W}^{LOST}$ is its difference compared to the lost work of the overall system (Table 4). Overall, $\approx 72\%$ of the offshore DMTM-GTW-CCU's available power ($\dot{W}^{MAX} = 1633.07$ MW) is wasted as lost work thanks to process irreversibilities.

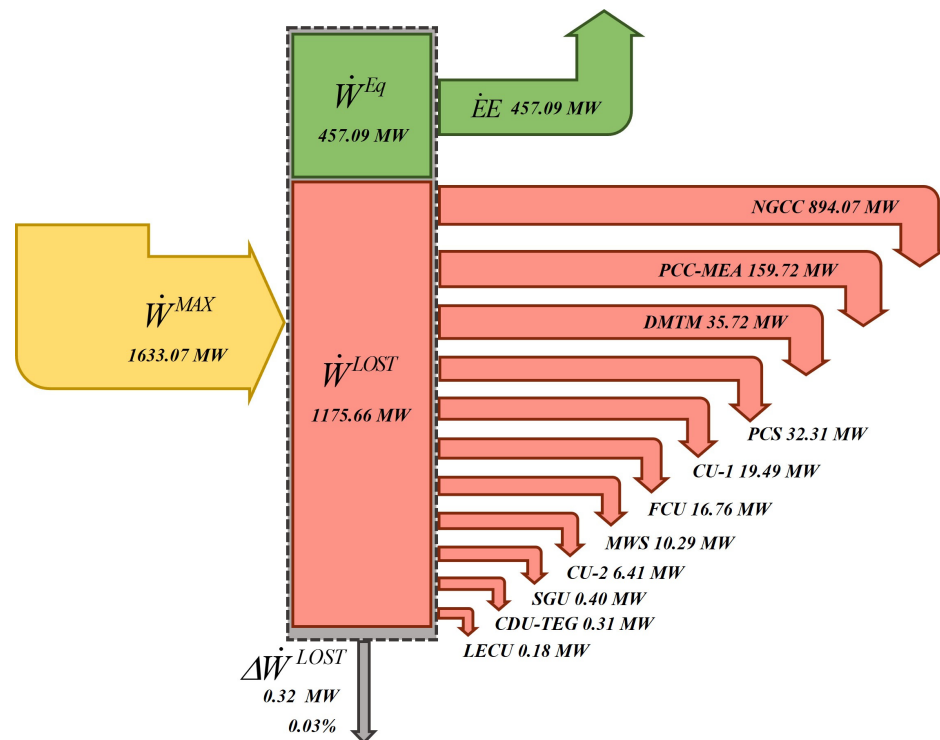


Figure 11. Lost work Sankey diagram ($\dot{E}E$: electricity; \dot{W}^{MAX} : maximum power; \dot{W}^{Eq} : equivalent power; \dot{W}^{LOST} : lost work; FCU: feed compression unit; DMTM-SCW: direct-methane-to-methanol in supercritical water; MWS: methanol–water separation system; LECU: light-ends combustion unit; NGCC: NG combined cycle; PCC-MEA: post-combustion capture with aqueous MEA; CU: CO₂ compression unit; CDU-TEG: CO₂ dehydration unit with TEG; SGU: stripping gas unit; PCS: primary cooling system).

The NGCC plant has the largest W^{LOST} (894.07 MW, 76.05% share), considering its extremely spontaneous combustion reactions. It is followed by the PCC-MEA (159.72 MW, 13.59% share), due to its columns/exchangers' head losses, the mass transfer finite potentials in the columns, the thermal approaches in the exchangers and stream mixing. The other sub-systems' lost work is modest, since these sub-systems are of low importance: DMTM-SCW (35.72 MW, 3.04% share), PCS (32.31 MW, 2.75% share), CU-1 (19.49 MW, 1.66% share), FCU (16.76 MW, 1.43% share), MWS (10.29 MW, 0.88% share), CU-2 (6.41 MW, 0.55% share), SGU (0.40 MW, 0.03% share), CDU-TEG (0.31 MW, 0.03% share) and LECU (0.18 MW, 0.02% share).

3.3. Comparison with the Literature

Hetland et al. [14] is a classical and essential reference on floating GTW-CCS. The authors carried out a theoretical GTW-CCS study evaluating PCC-MEA implementation downstream of a floating Siemens NGCC (450 MW). The authors pointed out that the floating GTW-CCS was technically feasible, although they did not consider intensification factors, as considered here, such as the EGR and CO₂-EOR stream dehydration (both are realistically necessary to radically reduce the CCS costs and to prevent CO₂ hydrate formation in the exported CO₂ stream). Additionally, they did not perform economic, thermodynamic or exergy analyses of the floating GTW-CCS. On the other hand, the present work filled these gaps as it considered a floating DMTM-GTW-CCU with a DMTM-SCW process coupled to gas-to-wire, achieving low emissions and producing methanol, wherein complete techno-economic, thermodynamic and lost work analyses were conducted. The present DMTM-GTW-CCU is able to generate 550 MW at low emissions and reasonable thermodynamic efficiency. Above all, it was demonstrated that the overall offshore DMTM-GTW-CCU process is potentially profitable, thermodynamically efficient and without environmental impacts.

In a recent work, using the same raw CO₂-rich NG conditions, Milão et al. [29] obtained thermodynamic efficiency of 35.5% for their offshore GTW-CCS (677 MW) overall process without considering DMTM, EGR and CO₂ dehydration. The present work found similar NGCC and PCC-MEA sub-system thermodynamic efficiencies and lost work but with differences in efficiency in the overall system (28% versus 35.5%). The underlying factor is that the DMTM addition upstream of the GTW-CCS in the present case made the offshore DMTM-GTW-CCU overall process more irreversible, consequently generating more lost work, despite the production of methanol. Moreover, the inclusion of EGR improves the PCC-MEA efficiency in the present case, reducing the lost work, while the inclusion of the TEG dehydration unit and the small stripping gas unit has the opposite effect, consuming power and generating lost work, resulting in lower overall thermodynamic efficiency of 28.0% for the present case. However, evidently, the present analysis is more complete and much more realistic.

These facts confirm that the proposal and the full analysis of the DMTM-GTW-CCU (with DMTM-SCW), as conducted here, constitute a novel study with reasonable contributions vis-à-vis the literature so far.

4. Conclusions

This work proposed and techno-economically and thermodynamically analyzed an innovative low-emission offshore DMTM-GTW-CCU process using CO₂-rich NG available at remote deep-water offshore sites as raw material. The DMTM-GTW-CCU partially converts methane from $\approx 6.5 \text{ MMSm}^3/\text{d}$ of CO₂-rich NG (CO₂ > 40%mol) into methanol (2.2 t/h) by conducting DMTM in supercritical water and then exports low-emission electricity (457.1 MW of net power) and liquid dry CO₂ as EOR fluid, bringing additional economic and environmental advantages. Offshore DMTM-GTW-CCU is an intensified power production process whose main intensification elements are (i) exhaust gas recycling (EGR), which reduces the flue gas flow rate while increasing its CO₂ content; (ii) post-combustion carbon capture via PCC-MEA from enriched flue gas; and (iii) high-pressure CO₂ dehy-

dration in CDU-TEG, which removes $\approx 94\%$ of the water from the CO₂-to-EOR stream to achieve the final content of ≈ 160 ppm-mol H₂O, preventing hydrate formation in EOR pipelines. EGR reduces the PCC-MEA investment and operational costs by lowering the column diameter/height, consequently increasing the DMTM-GTW-CCS' profitability. The process proves to be self-sufficient in process water, thus overcoming a fundamental aspect that would represent a serious shortcoming: at deep-water offshore sites, the continuous importation of water would be an obstacle to plant sustainability.

The PCC-MEA plant abates 491.3 t/h of the flue gas CO₂ ($\approx 90\%$). The captured CO₂ is compressed, dehydrated, compressed again and transported to EOR practically as pure dry CO₂ (CO₂ $\approx 99.97\%$ mol). This EOR stream is assumed to be traded at 1.5 bbl^{Oil}/t^{CO₂}, generating extra revenue. Considering the adopted economic assumptions, offshore DMTM-GTW-CCU with DMTM-SCW is economically feasible, with the following economic results: (i) 1544 MMUSD capital investment; (ii) 452 MMUSD/y cost of manufacturing; (iii) 820 MMUSD/y revenues (comprising methanol, electricity and CO₂-to-EOR); (iv) 1021 MMUSD NPV^{50years}; and (v) a 10 year payback time.

The Second Law analysis of the offshore DMTM-GTW-CCU overall system reveals 28% thermodynamic efficiency with $\approx 72\%$ of lost work, with the NGCC sub-system being the greatest lost work sink ($\approx 76\%$ share of overall lost work) due to the highly spontaneous gas turbine firing process. The second lost work sink lies in the PCC-MEA sub-system ($\approx 14\%$ share of overall lost work), while the DMTM-SCW system is the third lost work sink, with a $\approx 3\%$ lost work share, probably because the extension of the DMTM reaction is appreciably small to prevent methanol selectivity degeneracy. Thereby, the NGCC plant and PCC-MEA are the leading DMTM-GTW-CCU sub-systems that demand thermodynamic improvement in order to generate higher economic and environmental benefits. The consistency of the thermodynamic analysis was demonstrated through lost work sum crosschecks and lateral checks applying the alternative Second Law formula $T_0 \cdot \dot{S}^{UNIV}$ for the lost work (Table 4). In summary, this work demonstrates that the newly proposed DMTM-GTW-CCU process is techno-economically feasible, environmentally friendly, thermodynamically efficient and competitive with other gas-to-wire processes from the literature, as shown in Section 3.3.

5. Suggestions for Future Work

The results of the technical, economic and thermodynamic analyses of the offshore DMTM-GTW-CCU were obtained in the context presented in Tables 1 and 2. These results could be influenced by the variations in some parameters. Therefore, it is relevant to implement a sensitivity analysis varying the major factors that influenced the present work's results (especially the prices of NG, oil, methanol and electricity). It is worth mentioning that other factors, such as the geographical location and climate factors, could have influenced the results obtained in this work and should also be considered. In the same way, there are other different and important analyses that could be proposed to investigate the system, such as an exergy analysis of the process and an environmental impact analysis, among others.

Supplementary Materials: The following supporting information can be downloaded at: <https://www.mdpi.com/article/10.3390/pr12020374/s1>, Table S1 belongs to the Supplementary Materials file related to this article, which can be found in the online version.

Author Contributions: A.d.C.R.: Software, Writing—Original Draft, Validation, Investigation, Data Curation, Visualization, Writing—Review and Editing, Formal Analysis. O.d.Q.F.A.: Supervision, Project Administration, Writing—Review and Editing. J.L.d.M.: Conceptualization, Software, Methodology, Investigation, Supervision, Writing—Original Draft, Writing—Review and Editing, Visualization, Formal Analysis. All authors have read and agreed to the published version of the manuscript.

Funding: J.L.d.M. and O.d.Q.F.A. acknowledge financial support from CNPq-Brazil (313861/2020-0, 312328/2021-4) and from FAPERJ Brazil (E-26/200.522/2023, E-26/201.178/2021). A.d.C.R. acknowledges financial support from FAPERJ Brazil (E-26/203.508/2023).

Data Availability Statement: Data are contained within the article and Supplementary Materials.

Conflicts of Interest: The authors declare no conflicts of interest.

Abbreviations

CCS: Carbon Capture and Storage; CCU: Carbon Capture and Utilization; CDU-TEG: CO₂ Dehydration Unit with TEG; CE: Carnot Engine; CHP: Carnot Heat Pump; CU: Compression Unit; CW: Cooling Water; DMTM: Direct Methane-to-Methanol; EGR: Exhaust Gas Recycling; EOR: Enhanced Oil Recovery; FCU: Feed Compression Unit; FG: Flue Gas; GTW: Gas-to-Wire; HPS: High-Pressure Steam; HRSG: Heat Recovery Steam Generator; HVDC: High-Voltage Direct Current; LEC: Light-Ends Column; LECC: Light-Ends Combustion Chamber; LECE: Light-Ends Combustion Exchanger; LECU: Light-Ends Combustion Unit, LHV: Lower Heating Value; LPS: Low-Pressure Steam; MEA: Monoethanolamine; MWS: Methanol–Water Separation; MWSC: Methanol–Water Separation Column; NG: Natural Gas; NGCC: Natural Gas Combined Cycle; PCC-MEA: Post-Combustion Capture with Aqueous MEA; PCS: Primary Cooling System; SCW: Supercritical Water; SGU: Stripping Gas Unit; SW: Sea Water; TEG: Triethylene Glycol.

Nomenclature

AP, GAP	Net and gross annual profits (MMUSD/y)
CAP	Equipment capacity
C_{BM}	Bare module cost (MMUSD)
COL, COM	Costs of labor and of manufacturing (MMUSD/y)
CRM, CUT	Costs of raw materials and of utilities (MMUSD/y)
$DEPR$	Depreciation (MMUSD/y)
$\dot{E}E$	Electricity (MW)
FCI	Fixed capital investment (MMUSD)
G_i	Flow rate of i th feed stream (kmol/s)
\bar{H}, \bar{S}	Molar enthalpy (MJ/kmol), molar entropy (MJ/K·kmol)
K_i	Flow rate of i th product stream (kmol/s)
N_f	Number of feed streams (inputs)
N_p	Number of product streams (outputs)
NPV	Net present value (MMUSD)
P	Pressure (bar)
\dot{Q}, W	Heat duty, power (MW)
REV	Revenues (MMUSD/y)
T	Temperature (K)
Greeks	
η	Thermodynamic efficiency (%)
Superscripts	
CW, Eq, LPS	Cooling water, equivalent, low-pressure steam

References

- Neseli, M.A.; Ozgener, O.; Ozgener, L. Energy and exergy analysis of electricity generation from natural gas pressure reducing stations. *Energy Convers. Manag.* **2015**, *93*, 109–120. [[CrossRef](#)]
- de Freitas, V.A.; Vital, J.C.S.; Rodrigues, B.R.; Rodrigues, R. Source rock potential, main depocenters, and CO₂ occurrence in the pre-salt section of Santos Basin, southeast Brazil. *J. S. Am. Earth Sci.* **2022**, *115*, 103760. [[CrossRef](#)]
- Andrei, M.; Sammarco, G. Gas to wire with carbon capture & storage: A sustainable way for on-site power generation by produced gas. In Proceedings of the Abu Dhabi International Petroleum Exhibition & Conference, Abu Dhabi, United Arab Emirates, 13–16 November 2017. [[CrossRef](#)]
- Ojjiagwo, E.; Oduoza, C.F.; Emekwuru, N. Economics of gas to wire technology applied in gas flare management. *Eng. Sci. Technol. Int. J.* **2016**, *19*, 2109–2118. [[CrossRef](#)]
- Orisaremi, K.K.; Chan, F.T.S.; Chung, N.S.H. Potential reductions in global gas flaring for determining the optimal sizing of gas-to-wire (GTW) process: An inverse DEA approach. *J. Nat. Gas Sci. Eng.* **2021**, *93*, 103995. [[CrossRef](#)]
- Watanabe, T.; Inoue, H.; Horitsugi, M.; Oya, S. Gas to Wire (GTW) system for developing “small gas field” and exploiting “associated gas”. In Proceedings of the International Oil & Gas Conference and Exhibition in China, Beijing, China, 5–7 December 2006. [[CrossRef](#)]
- Sayed, S.; Massoud, A. Minimum transmission power loss in multi-terminal HVDC systems: A general methodology for radial and mesh networks. *Alex. Eng. J.* **2019**, *58*, 115–125. [[CrossRef](#)]
- Brito, T.L.F.; Galvão, C.; Fonseca, A.F.; Costa, H.K.M.; dos Santos, E.M. A review of gas-to-wire (GtW) projects worldwide: State-of-art and developments. *Energy Policy* **2022**, *163*, 112859. [[CrossRef](#)]

9. Zhou, D.; Li, P.; Liang, X.; Liu, M.; Wang, L. A long-term strategic plan of offshore CO₂ transport and storage in northern South China Sea for a low-carbon development in Guangdong province, China. *Int. J. Greenh. Gas Control* **2018**, *70*, 76–87. [CrossRef]
10. Roussanaly, S.; Aasen, A.; Anantharaman, R.; Danielsen, B.; Jakobsen, J.; Heme-De-Lacotte, L.; Neji, G.; Sødal, A.; Wahl, P.; Vrana, T.; et al. Offshore power generation with carbon capture and storage to decarbonise mainland electricity and offshore oil and gas installations: A techno-economic analysis. *Appl. Energy* **2019**, *233–234*, 478–494. [CrossRef]
11. Zhao, H.; Chang, Y.; Feng, S. Influence of produced natural gas on CO₂-crude oil systems and the cyclic CO₂ injection process. *J. Nat. Gas Sci. Eng.* **2016**, *35*, 144–151. [CrossRef]
12. Monson, C.C.; Korose, C.P.; Frailey, S.M. Screening methodology for regional-scale CO₂ EOR and storage using economic criteria. *Energy Procedia* **2014**, *63*, 7796–7808. [CrossRef]
13. Araújo, O.d.Q.F.; Reis, A.d.C.; de Medeiros, J.L.; Nascimento, J.F.D.; Grava, W.M.; Musse, A.P.S. Comparative analysis of separation technologies for processing carbon dioxide rich natural gas in ultra-deepwater oil fields. *J. Clean. Prod.* **2017**, *155*, 12–22. [CrossRef]
14. Hetland, J.; Kvamsdal, H.M.; Haugen, G.; Major, F.; Kårstad, V.; Tjellander, G. Integrating a full carbon capture scheme onto a 450 MWe NGCC electric power generation hub for offshore operations: Presenting the Sevan GTW concept. *Appl. Energy* **2009**, *86*, 2298–2307. [CrossRef]
15. Hachem, J.; Schuhler, T.; Orhon, D.; Cuif-Sjostrand, M.; Zoughaib, A.; Molière, M. Exhaust gas recirculation applied to single-shaft gas turbines: An energy and exergy approach. *Energy* **2022**, *238*, 121656. [CrossRef]
16. Li, H.; Ditaranto, M.; Yan, J. Carbon capture with low energy penalty: Supplementary fired natural gas combined cycles. *Appl. Energy* **2012**, *97*, 164–169. [CrossRef]
17. Li, H.; Ditaranto, M.; Berstad, D. Technologies for increasing CO₂ concentration in exhaust gas from natural gas-fired power production with post-combustion, amine-based CO₂ capture. *Energy* **2011**, *36*, 1124–1133. [CrossRef]
18. Ahmadi, M.A.; Soleimani, R.; Bahadori, A. A computational intelligence scheme for prediction equilibrium water dew point of natural gas in TEG dehydration systems. *Fuel* **2014**, *137*, 145–154. [CrossRef]
19. Zakaria, Z.; Kamarudin, S.K. Direct conversion technologies of methane to methanol: An overview. *Renew. Sustain. Energy Rev.* **2016**, *65*, 250–261. [CrossRef]
20. Zhang, Q.; He, D.; Li, J.; Xu, B.; Liang, Y.; Zhu, Q. Comparatively high yield methanol production from gas phase partial oxidation of methane. *Appl. Catal. A Gen.* **2002**, *224*, 201–207. [CrossRef]
21. Holmen, A. Direct conversion of methane to fuels and chemicals. *Catal. Today* **2009**, *142*, 2–8. [CrossRef]
22. Han, B.; Yang, Y.; Xu, Y.; Etim, U.; Qiao, K.; Xu, B.; Yan, Z. A review of the direct oxidation of methane to methanol. *Chin. J. Catal.* **2016**, *35*, 1206–1215. [CrossRef]
23. Ravi, M.; Ranocchiari, M.; van Bokhoven, J.A. The Direct Catalytic Oxidation of Methane to Methanol—A Critical Assessment. *Angew. Chem. Int. Ed.* **2017**, *56*, 16464–16483. [CrossRef]
24. Savage, P.E.; Li, R.; Santini, J.T. Methane to methanol in supercritical water. *J. Supercrit. Fluids* **1994**, *7*, 135–144. [CrossRef]
25. Zhang, F.; Li, Y.; Liang, Z.; Wu, T. Energy conversion and utilization in supercritical water oxidation systems: A review. *Biomass Bioenergy* **2022**, *156*, 106322. [CrossRef]
26. Lee, J.H.; Foster, N.R. Direct partial oxidation of methane to methanol in supercritical water. *J. Supercrit. Fluids* **1996**, *9*, 99–105. [CrossRef]
27. Le Guennec, Y.; Privat, R.; Jaubert, J.-N. Development of the translated-consistent tc-PR and tc-RK cubic equations of state for a safe and accurate prediction of volumetric, energetic and saturation properties of pure compounds in the sub- and super-critical domains. *Fluid Phase Equilib.* **2016**, *429*, 301–312. [CrossRef]
28. Le Guennec, Y.; Privat, R.; Lasala, S.; Jaubert, J.-N. On the imperative need to use a consistent α -function for the prediction of pure-compound supercritical properties with a cubic equation of state. *Fluid Phase Equilib.* **2017**, *445*, 45–53. [CrossRef]
29. Milão, R.d.F.D.; de Medeiros, J.L.; Interlenghi, S.F.; Araújo, O.d.Q.F. Low-emission Gas-to-Wire with thermodynamic efficiency: Monetization of carbon dioxide rich natural gas from offshore fields. *Gas Sci. Eng.* **2023**, *115*, 205021. [CrossRef]
30. Ott, J.; Gronemann, V.; Pontzen, F.; Fiedler, E.; Grossman, G.; Kersebohm, K.B.; Weiss, G.; Witte, C. Methanol—An Industrial Review by Lurgi GmbH, Air Liquide GmbH and BASF AG. In *Ullmann's Encyclopedia of Industrial Chemistry*; Wiley-VCH Verlag GmbH & Co. KGaA: Weinheim, Germany, 2012.
31. Chebbi, R.; Qasim, M.; Jabbar, N.A. Optimization of triethylene glycol dehydration of natural gas. *Energy Rep.* **2019**, *5*, 723–732. [CrossRef]
32. Siemens Energy. SGT-A35 Aeroderivative Gas Turbine. Available online: <https://www.siemens-energy.com/global/en/offerings/power-generation/gas-turbines/sgt-a30-a35-rb.html> (accessed on 2 September 2022).
33. Følgesvold, E.; Skjefstad, H.; Riboldi, L.; Nord, L. Combined heat and power plant on offshore oil and gas installations. *J. Power Technol.* **2017**, *97*, 117–126.
34. GE. Aeroderivative LM2500 Gas Turbine (50Hz): Fact Sheet. 2019. Available online: https://www.ge.com/content/dam/gepower/global/en_US/documents/gas/gas-turbines/aero-products-specs/lm2500-50hz-fact-sheet-product-specifications.pdf (accessed on 2 September 2022).
35. Kloster, P. Energy Optimization on Offshore Installations with Emphasis on Offshore Combined Cycle Plants. In Proceedings of the SPE Offshore Europe Oil and Gas Conference and Exhibition, Aberdeen, UK, 7–10 September 1999; Society of Petroleum Engineers: Aberdeen, UK, 1999. [CrossRef]

36. GE. LM2500+G4 Marine Gas Turbine. 2021. Available online: <https://www.geaviation.com/sites/default/files/datasheet-lm2500plusg4.pdf> (accessed on 2 September 2022).
37. Oh, S.-Y.; Binns, M.; Cho, H.; Kim, J.-K. Energy minimization of MEA-based CO₂ capture process. *Appl. Energy* **2016**, *169*, 353–362. [[CrossRef](#)]
38. Araújo, O.d.Q.F.; de Medeiros, J.L. Carbon capture and storage technologies: Present scenario and drivers of innovation. *Curr. Opin. Chem. Eng.* **2017**, *17*, 22–34. [[CrossRef](#)]
39. Liu, G.; Zhu, L.; Hong, J.; Liu, H. Technical, Economical, and Environmental Performance Assessment of an Improved Triethylene Glycol Dehydration Process for Shale Gas. *ACS Omega* **2022**, *7*, 1861–1873. [[CrossRef](#)] [[PubMed](#)]
40. Turton, R.; Bailie, R.C.; Whiting, W.B.; Shaeiwitz, J.A. *Analysis, Synthesis and Design of Chemical Processes*, 4th ed.; Prentice Hall: Columbia, MI, USA, 2012.
41. Towering Skills. 2023. Available online: <https://toweringskills.com/financial-analysis/cost-indices/> (accessed on 20 September 2023).
42. Windén, B.; Chen, M.; Okamoto, N.; Kim, D.K.; McCaig, E.; Sheno, A.; Wilson, P. Investigation of offshore thermal power plant with carbon capture as an alternative to carbon dioxide transport. *Ocean Eng.* **2014**, *76*, 152–162. [[CrossRef](#)]
43. EIA. U.S. Energy Information Administration. *Natural Gas*. 2023. Available online: <https://www.eia.gov/dnav/ng/hist/rngwhhdm.htm> (accessed on 20 September 2023).
44. CHEMANALYST. 2023. Available online: <https://www.chemanalyst.com/Pricing-data/methanol-1> (accessed on 20 September 2023).
45. Statista. Petroleum & Refinery. 2023. Available online: <https://www.statista.com/statistics/262861/uk-brent-crude-oil-monthly-price-development/> (accessed on 20 September 2023).

Disclaimer/Publisher's Note: The statements, opinions and data contained in all publications are solely those of the individual author(s) and contributor(s) and not of MDPI and/or the editor(s). MDPI and/or the editor(s) disclaim responsibility for any injury to people or property resulting from any ideas, methods, instructions or products referred to in the content.